Review of the paper "Can models robustly represent aerosol–convection interactions if their cloud microphysics is uncertain?", authored by B. White, E. Gryspeerdt, P. Stier, H. Morrison, and G. Thompson.

The authors have drawn a pretty grim picture of the situation with the description of microphysics in cloud resolving models using bulk parameterization schemes. Two known bulk parameterization schemes referred to as "MORR" (Morrison and Milbrandt (2011) and "THOM" (Thompson et al. (2004, 2008)) were tested by simulation of 3 case studies with different type of convection: from shallow convection to a supercell storm. The simulations were performed at a priory given droplet concentrations of 100 cm-3, 250 cm-3 and 2500 cm-3. A dramatic difference between parameters of simulated clouds (cloudiness, simulated precipitation, etc.) and observations is demonstrated. A huge difference in cloud microphysical structure simulated by these two schemes is reported. Both bulk schemes turned out to be insensitive to droplet concentration. So, the difference in results are related to the differences in the bulk-parameterization schemes.

My particular comments and remarks are the following.

1. The finding about high diversity of cloud microstructure and precipitation produced by different bulk schemes is not new. Any intercomparison study shows such diversity. The insensitivity of most bulk schemes to aerosols (and to droplet concentration) also well known. For instance, application of different bulk -parameterization schemes to simulation of hurricane Irene (2011), including "MORR" and "THOM", led to a TC with maximum wind varying from 30 m/s to 70 m/s (Khain et al., 2015; Khain et al. 2016-Atmospheric Research 167, 129–145). In these studies insensitivity of bulk schemes to aerosols was also demonstrated and an possible explanation of such insensitivity is presented.

We agree with Reviewer 1 that it has been shown that different microphysics schemes produce a high diversity of cloud development and precipitation. We have significantly revised our introduction to show this more explicitly, and in doing so have included the references and possible explanations suggested by the Reviewer. This is in P1 L20 through P8 L4 of our revised manuscript.

We certainly do not intend to claim this in itself as a new result. However, we confirm this in a single modelling framework, for three different cloud and environment types, in three different simulation types (one performed with meteorological data, one idealised supercell using open boundaries, one warm-phase cumulus case with periodic boundaries). This is necessary to show before presenting our main results: (a) that the largest source of uncertainty (or variability) between simulations is in the choice of microphysics scheme, and that any aerosol effect is secondary, and (b) that the response of the hydrometeors to CDNC perturbations differs strongly not just between microphysics schemes but also that the inter-scheme variability differs between cases of convection

Although they do not always respond to aerosol as strongly as bin schemes, bulk schemes have been shown to be sensitive to aerosol, e.g. Morrison & Grabowski 2011, who found an ice-phase response to aerosol. Indeed, a similar mechanism was later confirmed in bin-scheme simulations by Fan et al. 2013. Further, Kalina et al. 2014 found that autoconversion of cloud water to rain decreased under polluted conditions and, subsequently, near-surface rain and hail particles increased in size due to enhanced collection of cloud droplets. Although the sensitivity of the bulk schemes used in the current study to perturbations in cloud droplet numbers was secondary to the sensitivity in cloud and precipitation

development dependent on the choice of bulk scheme, we nevertheless feel this is a significant result to present in the context of multiple cloud types and types of simulation, given that bulk microphysics schemes remain in wide use.

Futher, in idealised supercell simulations using the WRF-SBM, we find the same order of magnitude of aerosol effect as in our bulk scheme simulations, and uncertainty due to microphysics scheme still dominates aerosol effects (Figure S4 in the Supplement).

We present in Figure S1 in the Supplement joint histograms for our Congo basin simulations of cloud top height in convective updraughts (columns identified with vertical velocities greater than 1 ms^{-1}) and the radius of the updraughts, as identified by running a connected-components labelling algorithm on the field of identified updraughts. Figure S1 shows that the most significant dynamical difference comes from choice of microphysics scheme: the Morrison scheme has a tendency towards higher frequencies of wider updraught radii with higher cloud tops than the Thompson scheme.

We note that the updraught dynamics in the Congo simulations respond very differently to aerosol. Figure R2 shows the difference between the joint histograms for the polluted and pristine cases for each microphysics scheme, respectively. While MORR shows little consistent aerosol response, THOM shows consistently lower frequencies of occurrence of all updraught radii and a reduced frequency of occurrence of the highest updraught tops under polluted conditions, with an increased frequency of occurrence of small updraught radii with lower cloud tops. Therefore, a consistent aerosol response is observed in THOM, resulting in smaller and lower convective updraughts (i.e. weakened convection under polluted conditions). Interestingly, both of these effects contradict the findings of Morrison & Grabowski 2011, who found an ice-phase response to aerosol in which cloud top heights and anvil ice mixing ratios increase under polluted conditions due to increased freezing of larger numbers of cloud droplets and subsequent higher ice particle concentrations with smaller sizes and reduced fall speeds. However, we note again that we consider different values of CDNC / CCN (and responses may be nonmonotonic, Kalina et al. 2014), and different case of convection (indeed, our 10-day Congo simulation covers many convective lifecycles). This combined with the findings already presented in our study, leads us to suggest that it is not certain that a consistent response in a different case of convection and with different CDNC values would be expected.

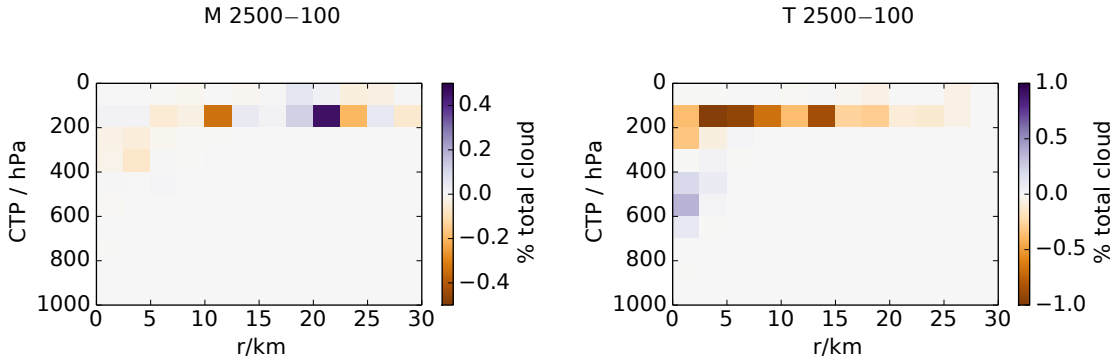

Figure R2: *Congo case: difference in joint histograms of updraught radius and cloud top pressure at the top of the cloudy updraughts between the polluted and pristine cases for MORR (left) and THOM (right).*

We have included Figure R2 in the revised paper and the relevant discussion Is on P11 L11-30.

2. The finding that description of the autoconversion is of crucial importance for correct simulation of cloud microphysics is also not new. For instance, Gilmore and Straka (2008) showed that the most formulae for autoconversion used in bulk schemes are applicable to the initial stage of the first raindrop formation only, and that the rates predicted by these formulae differ by orders of magnitude. There are many other studies showed dramatic sensitivity of cloud microstructure to the scheme of autoconversion. So, the new information in the paper is that these conclusions are confirmed in investigation of these two particular bulk schemes.

We thank Reviewer 1 for the Gilmore & Straka reference which helps to give context to our findings. We have included this reference in our Results (P18 L10) and Conclusions (P25 L24) section.

We do not claim our finding that cloud structure is sensitive to autoconversion representation to be a new result. Rather, we find that autoconversion is sufficient to explain some of the key differences between the clouds simulated by the two bulk microphysics schemes, namely those in the liquid phase. Further, we show that aerosol effects are dominated by the response of the autoconversion process for this case. Li et al. (2015, JAS) also showed that a slower autoconversion process along with a stronger accretion process explains the Morrison scheme's higher cloud fraction than the Thompson scheme for a similar rain mixing ratio.

This is in part a finding in itself that addresses Reviewer 1's comment 4. It is because we were trying to understand which processes were significant to the differences in cloud microstructure in the context of comparing these two schemes that we investigated the autoconversion representation. Indeed, we cannot say in the cases we consider which is the more 'correct' representation. We rather highlight that some of the differences we observe between the schemes, in some of the types of convection, can be almost entirely attributed to the representation of autoconversion, and that differences in other processes between the two schemes are secondary.

Further, our tests highlighted the difference between the MORR and THOM schemes in the interplay and relative importance of the autoconversion and accretion processes: the Thompson scheme can produce surface rain from autoconversion alone (although two orders of magnitude less than when rain can also accrete cloud water), showing that autoconversion acts almost like a 'seed' for rain production in this scheme, after which accretion takes over the rain production process. However, in the Morrison scheme, when autoconversion is allowed to occur but accretion of cloud water by rain is prevented, precipitation shuts down, thus indicating that both autoconversion and accretion are necessary processes for warm rain production in MORR.

This is discussed in our Results section.

3. The authors illustrate vertical profiles of mass contents of different hydrometeors averaged over the entire computational area. As a result, all information concerning the microphysical structure of clouds simulated by different schemes turns out to be lost, at least for specialists in cloud microphysics. It is necessary to present vertical profiles of maximum values of the mass contents. The profiles of cloud averaged values would be also useful. These figures should be accompanied by corresponding comments and analysis.

It is important to include the profiles averaged over the entire domain, because (at least for larger-scale impacts) this illustrates the difference in the bulk properties and accounts for differences in total cloud cover, which in turn has implications for radiative effects and

feedbacks. This is especially important in our Congo simulations, where differences in the ice-phase microphysics between the schemes lead to large differences in the ice cloud fraction, which will in turn have a significant radiative impact.

We agree with Reviewer 1 that it would also be useful to see the mean in-cloud properties, and changes thereof. We thus now include condensate-averaged profiles for each hydrometeor type in order to identify not only the bulk impact of changes in CDNC in each simulation but also the bulk properties of the cloud in each convective study. We note that in the idealised supercell case and the RICO LES case there is little difference between the domain-mean profiles and the hydrometeor class-mean profiles.

Comments and analysis of these new profiles have been included in our revised manuscript. The relevant Figures are Figures 6,7,8,9,11,12.

An example of the condensed-point average profiles is provided in our response to Reviewer 2's comment 12.

However, we do not agree that showing domain-maximum values is useful, because the maximum values of the mass contents represent just one point in the entire domain and can lead to improper conclusions, especially in our Congo simulation where multiple cloud types exist in the same domain but do not necessarily interact.

4. The lack of physical interpretation of results is another drawback of the study. For instance, Fig. 6 and Fig. 7 show that in simulations CONGO - T250, T-2500 maximum cloud water content (i.e. small cloud droplets) is located at the surface. One gets the impression that the entire boundary layer is filled with tiny droplets (but not with raindrops). What can be physical mechanisms leading to this very strange effect? The comment concerning the lack of interpretation is related to most figures.
The low cloud extending down to near-surface regions is indeed a strange effect. However, it is produced consistently in all simulations (including the simulation performed with WRF SBM microphysics, see Figures S2 and S3 in the Supplement now included with this response). We note also that in our WRF-SBM simulation (Figures S1 and S2 in the Supplement) the warm cloud mass has significantly greater domain-mean values than the M250 case. We believe this difference is because, as we have shown (our Figure 16), the cloud mass in the M250 case is removed through autoconversion to rain, whereas this does not occur in the T250 case (or indeed the SBM). When the THOM autoconversion is used in the equivalent MORR simulations (or when autoconversion is turned off completely in MORR), the cloud droplets persist as in THOM. Although we have not tested the equivalent process in the SBM simulation presented in this response, we suggest that lack of autoconversion (or, stronger autoconversion than THOM but weaker than that in MORR) is responsible for the persistence of the cloud droplets in THOM. That all schemes produce the warm cloud mass, but some configurations rain it out if the autoconversion rate is fast enough, leads us to suggest that it is not the Thompson scheme per se which is responsible for producing the low-level cloud mass, but rather the meteorological conditions present in which these simulations are performed. We provide in our response to Reviewer 2's comment 21 a figure (Fig. R4 in the response to Reviewer 2) figures and further discussion on the presence of this low warm cloud mass.

We have now included such comments on the presence of the warm cloud mass in our Results (P20 L10-16) section.

However, we disagree with Reviewer 2's comment that there is a general lack of interpretation. In the liquid cloud (warm cloud mass in the south of the Congo domain and the cloud in the RICO simulations) the differences can be attributed to the autoconversion, as we have already shown in our tests and describe in the discussion of our figures. In the deep convective cloud (where ice processes can occur), much of the difference between the schemes can be attributed to differences in the classification of frozen particles, which we have already discussed at length.

In addressing the Reviewer's comments on lack of interpretation, we have now performed further simulations which test the autoconversion of cloud ice to snow in the two schemes. These are presented and discussed in our revised manuscript and can be found from P20 L17 to P21 L2.

5. The section of Conclusions is weak. The authors stress that their key findings are a) "A key finding is that the simulated hydrometeor classes differ significantly between microphysics schemes" b) "Another key finding is that the difference between the hydrometeor classes simulated by each microphysics scheme varies between cases of convection." c) Another key finding is that the cloud morphological difference and the difference in the hydrometeors between different schemes is significantly larger than that due to CDNC perturbations.

As it was said above, all these findings are not new.
I would recommend to rewrite conclusions by adding more detailed analysis of results and recommendations of the ways to improve the schemes.
We present the new results that the way in which the schemes differ from each other between cases of convection is not systematic, and further that their response to aerosol also differs non-systematically.

By performing simulations within a single modelling framework we reduce much of the uncertainty in comparing results from different microphysics schemes noted by Khain 2015, such as orography, boundary layer parameterization, etc. We note that we have only performed real-data simulations in one region over one 10-day period in August 2007 and therefore would not expect our results to be exactly the same in another region or in another season, where orography, large-scale meteorology, and cloud type would be different from that present in our simulations. However, our main result is that cloud impacts from choice of microphysics scheme far exceed cloud impacts from CDNC perturbations in every case we consider, and therefore we would expect that even though the cloud development and response to CDNC would clearly be different in another regime, the uncertainty due to choice of microphysics scheme would still dominate.

We have rewritten our Conclusions, and put our results in the context of a wider body of previous work. These can be found in the revised manuscript from P21 L21 through P26 L4.

We stress that without observations it is difficult to suggest ways to improve the schemes. However, we have now performed extra tests to explain the processes which lead to the large differences in upper-level ice in the Congo simulations. This is discussed in our Results section from P20 L18 through P21 L2, along with suggestions as to how the schemes could be improved.

Further, we also find the same persistent upper-level ice in our WRF-SBM Congo simulations, which we present in the Supplement. Although the focus of this paper is not to provide a comparison of bin vs bulk schemes, we show that the differences resulting from

conversion of one ice category into another is a limitation of any scheme whether bin or bulk which uses fixed ice categories. Our results support the argument that ice phase processes may be better represented if developments in microphysics schemes starts to move away from the use of fixed ice categories.

Review of the ACP manuscript “Can models robustly represent aerosol–convection interactions if their cloud microphysics is uncertain?” by White et al. The authors used the WRF model coupled with two double-moment bulk microphysics scheme to perform cloud system-resolving simulations of convection in the Congo basin, an idealized supercell, and a case of shallow cumulus convection, and tested the sensitivity of the simulated hydrometeors and precipitation to the microphysics scheme and to CDNC perturbations. The authors showed the simulations are sensitive to microphysics parameterizations much more than CDNC, which has been showed in previous studies but this study highlighted this point to imply aerosol effects are the secondary compared with the uncertainty in cloud parameterization. They further examined the shallow cumulus convection case and found that representation of autoconversion is the dominant factor that drives differences in rain production. The paper is generally written clearly but there are confusing sentences. They are some perspectives that can not be well justified physically such as saying the aerosol-cloud interactions in their study represent the upper limit.
The major problem is that their main point is based on an assumption that those twomoment schemes well represent the aerosol-cloud interactions, which is not the case based on the many past studies and a recent review paper by Khain et al 2015. Twomoment schemes have significant limitations in aerosol-cloud interaction process parameterizations such as nucleation, diffusional growth, and sedimentation, etc (detailed Khain et al. 2015). The paper did not really address the question “Can models robustly represent aerosol–convection interactions if their cloud microphysics is uncertain”, so that the title needs to be changed. More literature survey is needed, especially about those studies comparing different microphysics schemes and their responses to CCN or CDNC. Those studies need to be discussed in the introduction and the relevant places in the paper, especially about some important points on the problems with the parameterizations of some specific microphysics processes in the bulk schemes. Therefore, the paper needs major revisions to be accepted as a publication in ACP.

We thank Reviewer 2 for their thoughtful and constructive comments, which we have found useful in helping us to clarify our manuscript for the reader.

We present this study as an illustration that model uncertainty in cloud impacts arising from choice of microphysics scheme can far outweigh any aerosol effects observed within a single scheme, and that this result holds for case study simulations consisting of many cloud lifecycles, for idealised simulations with open boundaries, for idealised simulations with periodic boundaries, and (by nature of the cases used in our study) across different types of convection with their inherently different response to aerosol.

Our choice to use bulk microphysics schemes is twofold; first, they remain in wide use in the community (often for practical reasons of computational cost) and even represent state-of-the-art implementation in global models, which have historically relied on much cruder microphysics representations, and second (most importantly) there is currently only one bin microphysics scheme implemented in the public version of WRF (although it comes in two slightly different versions, a ‘full’ and ‘fast’ version which differ in the number of ice categories used) and thus our study would be impossible to perform within a single modelling framework had we opted to use bin schemes.

Specific comments:

1. The title needs to be changed. It is relevant but the authors did not conduct an unique study to really address this question. The two-moment schemes can not robustly represent aerosol–convection interactions due to the limitations in representing the most relevant processes as detailed in Khain et al. 2015. If a bin scheme is used, you might end up with similar magnitudes of aerosol indirect effects as the differences among different microphysics schemes. In addition, for specific case simulations, one can not really reveal how it is impacted by aerosols by conducting simulations with realistic aerosols/chemistry configuration. Any aerosol properties and spatial distribution change could change cloud and precipitation.

We have updated the title to emphasize our main result:
‘Uncertainty from choice of microphysics scheme in convection-permitting models significantly exceeds aerosol effects’.

Regarding the reviewer’s comments on the use of a bin scheme:
We have now performed simulations using the HUJI spectral bin microphysics scheme (SBM) implemented in WRFv3.6.1 (note that this is a newer version of WRF than used in the Morrison and Thompson simulations presented in the paper). We do not wish to further extend the paper to include discussion of the impacts of bin vs bulk microphysics in these cases (because the main aim of this particular paper is to highlight within a single paper and by using a single modelling framework the large uncertainty in many case study and GCM simulations that can result from any given combination of microphysics scheme, type of convection, and given CDNC value or prescribed CCN profile). However, we now present our bin scheme results in a supplement to our paper (Figures S2, S3 and S4) because we believe our results to be of interest. We find that the uncertainty due to choice of microphysics scheme still dominates any aerosol response within each scheme in the cases we test, regardless of whether a bin or bulk scheme is used.

2. P1, L21-22: aerosol can affect through aerosol radiative effects as well.
We did not intend our phrasing to imply that the only effect that aerosol has on convection is an indirect effect through cloud microphysics. We have reworded the sentence now on P1 L22 – P2 L1:
"One major way that aerosols can influence the properties of deep convection is through their effect on cloud microphysics."

3. P1, L24: Albrecht, 1989 actually showed the suppression of precipitation but for warm clouds. So, the sentence is not accurate.
We thank the reviewer for finding our omission of "warm-phase" in this sentence, and have corrected our sentence to "warm-phase precipitation", now on P2 L3.

4. P2, L29: "Until recently" should be deleted.
We replace "until recently" with "traditionally" (now on P5 L20), as it is only in recent years that schemes have started to move away from discrete ice categories (Morrison & Grabowski 2008, Harrington et al. 2013, Morrison & Milbrandt 2015), and we wish to make it clear to the reader that this is a relatively new and important development.

5. P4, L19-25, these sentences could be misleading. First, it is not clear what the authors mean by saying "the response of different microphysics schemes to perturbations in prescribed cloud parameters". Second, some past studies showed qualitatively different aerosol impact for different cloud types, with a purpose of illustrating a point that aerosol impacts depend on cloud type and dynamical and thermodynamic conditions of each case. So it is misleading to describe a study without giving information about cloud types or specific dynamical and thermodynamic environment. For example, the description about Fan et al. 2012 about aerosol reducing precipitation is not correct. The study did two different cloud cases over the eastern China – one deep convective cloud case with warm cloud base and weak wind shear and the other a winter stratiform cloud case, with aerosol increased precipitation for the former but reduced precipitation for the latter.
We thank the reviewer for pointing out that this was not clear to the reader.

We have heavily revised our introduction and included more detailed discussion on aerosol response in bin and bulk schemes, noting the convective regimes and large-scale environments used in each study. The paragraph P4 L19-25 has now been removed.

6. P5, L3: cloud and precipitation responses > cloud and precipitation responses to perturbation of CDNC
We thank the reviewer for noticing this omission and have amended our text (now on P8 L3) accordingly.

7. P5, L25: Khain and Lynn 2009 is not s study with specified CDNC. CDNC is prognostic in the bin model they used.
We thank the reviewer for this correction and have amended our text.

8. P6, first paragraph, RRTM and Goddard schemes only talk hydrometeor mass from microphysics calculation (Goddard shortwave scheme takes prognostic CDNC as well). The microphysics-radiation coupling does not account for particle size changes, which means some aerosol effects are missing in those studies.
We agree with the reviewer and we also note that the microphysics-radiation coupling is only between cloud water and ice, and none of the other frozen species. This missing aerosol effect may have an especially important impact in our Congo simulations, where the Morrison scheme develops and retains significant amounts of upper-level ice, whereas the Thompson scheme converts nearly all the ice to snow (see Figures in our response to Reviewer 1), which the radiation scheme will not see. This could have significant radiative flux and feedback impacts (Thompson 2015, Atmospheric Research), which in itself originates from the use of somewhat arbitrarily defined ice categories (e.g. if the size parameter at which cloud ice is converted to snow is changed, a bulk mass of cloud ice is removed from the radiatively-coupled ice category and moved into the non-radiatively coupled snow category).

We have included these important points in our Discussion and Conclusions of the Congo basin results, P24 L6-15.

9. Figure 3, the color scheme needs to be changed. The color difference is too little even between 0 and 100 mm.
We have changed the colour scale of this Figure to a scale which more clearly shows the large difference in accumulated rain over the 10-day period between the models and observations. The new Figure is shown below in Figure R1.

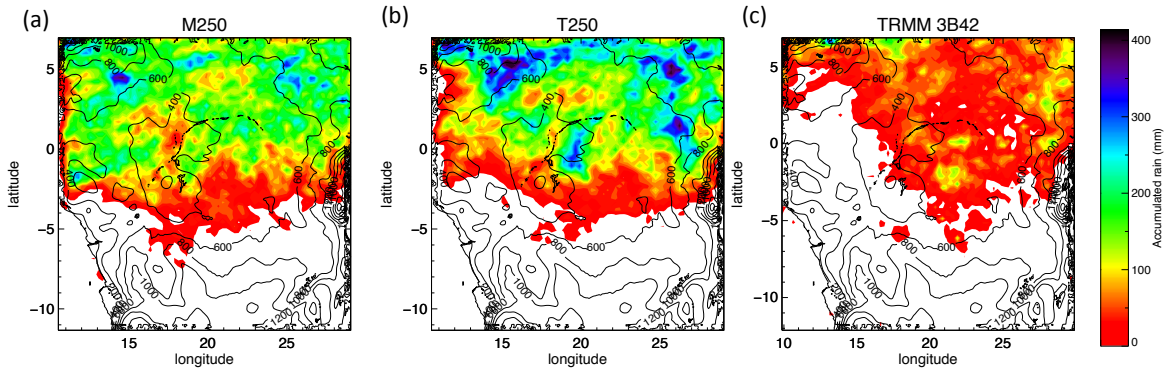

Figure R1: *Congo case: accumulated surface precipitation (mm) from 01 to 10 August 2007 in the Congo basin, showing data from (a) CONGO-M250, (b) CONGO-T250 and (c) observations from the TRMM 3B42 gridded 3-hourly mean merged precipitation product. The simulation data shown in this Figure has been coarsened to the 0.25 degree spatial resolution of the TRMM product.*

10. Figure 5, why compare with the climatology data? This is just a 10-day run, how should we expect it represent the climatology?

There were so few CloudSat overpasses during the 10-day period that the resulting histogram is very noisy compared to the model data, albeit qualitativey very similar to the climatology (see figure R2 below compared to Figure 5 in the paper). This is why we originally used the observed climatology to construct Figure 5. At Reviewer 2's suggestion, we have replaced Figure 5 in our manuscript with the histogram showing 10 days of CloudSat data, Figure R2 below.

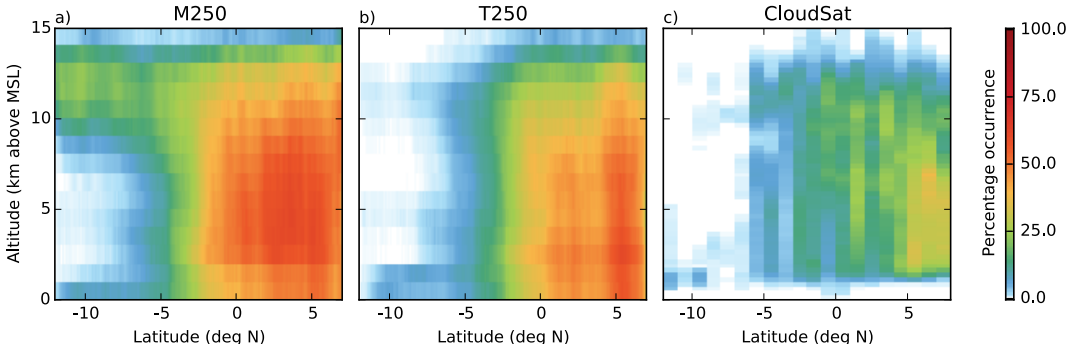

Figure R2: *Congo case: 10-day histogram for the period 1 – 10 August 2007 of model reflectivities derived from hydrometeor fields passed through the Quickbeam radar simulator, thresholded at values greater than -20 dBZ for (a) CONGO-M250, (b) CONGO-T250, and (c) the CloudSat 2B-GEOPROF product. In (a) and (b) the models have been sampled at the times of the nearest CloudSat overpasses.*

11. P. 9 L5-7, this sentence is confusing. Need to be clarified.

We have now expressed this sentence more clearly (P12 L22):

"The largest reflectivity values produced by the model occur in the convective region in the north of the domain, where the largest reflectivity values are detected by the satellite radar.'

12. P. 9, L19: domain averaged cloud water in T250 is 140 times larger than M250. Something could be wrong here. Can you plot the cloudy-point average for cloud water mass total hydrometeor mass to check if they make sense? What is the maximum cloud water mass in T250 and M250, respectively?

This is correct in the domain-average profile, because the shallow warm cloud in the M250 case precipitates out, whereas it persists in the T250 case. This leads to a significant difference in the domain-averaged cloud water mass, because there are many zero points in the M250 case which contain cloud water in T250 (see also our response, including figure, to Reviewer 2's comment 21)

Considering the cloudy-point (condensed-point) averages, we see a similar response in behaviour (increased cloud water mass in T250 compared to M250), except the magnitude is reduced because the profiles are normalized by number of points with condensed water. The condensed-point average profiles show qualitatively similar behavior in all cloud species to the domain-mean profiles (Figure R3), except cannot represent absolute changes in the number of cloudy / condensed points between the simulations.

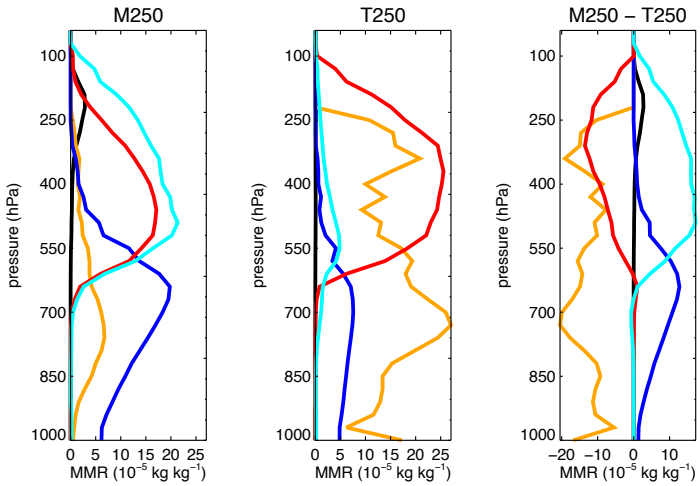

Figure R3: *Congo case: Cloud-and-condensed-point mean vertical profiles of difference in hydrometeor mass mixing ratios between the polluted and pristine cases, averaged over the 10 days of the Congo simulation for the Morrison scheme (left), Thompson scheme (centre) and difference between the two (right).*

We note also that in our WRF-SBM simulation (Figures S2 and S3 in the supplement provided with this response) the same warm cloud mass is present and has significantly greater domain-mean values than the M250 case. We believe this difference is because, as we have shown (our Figure 16), the cloud mass in the M250 case is removed through autoconversion to rain, whereas this does not occur in the T250 case or in the SBM.

13. Figure 6, this figure need to be replotted to show differences of other hydrometeor mass clearly. Right now, only cloud water differences can be seen clearly. I would use different panels for different hydrometeors.
We agree with the reviewer that this is a difficult figure to show all hydrometeor masses clearly whilst also showing the significant difference in cloud masses between the two schemes. However, we feel that using different panels for the different hydrometeors could confuse the reader, as this is not done for any other such figures. We now present the following figure, which shows all the hydrometeor classes on the same figure, as for all other such profiles in the paper, but uses a logarithmic horizontal axis even in the difference plot. This makes clear to the reader the differences of all the hydrometeor classes, not just the cloud water, whilst also showing that the difference in cloud water between the two schemes is an order of magnitude greater than between the other hydrometeor classes.

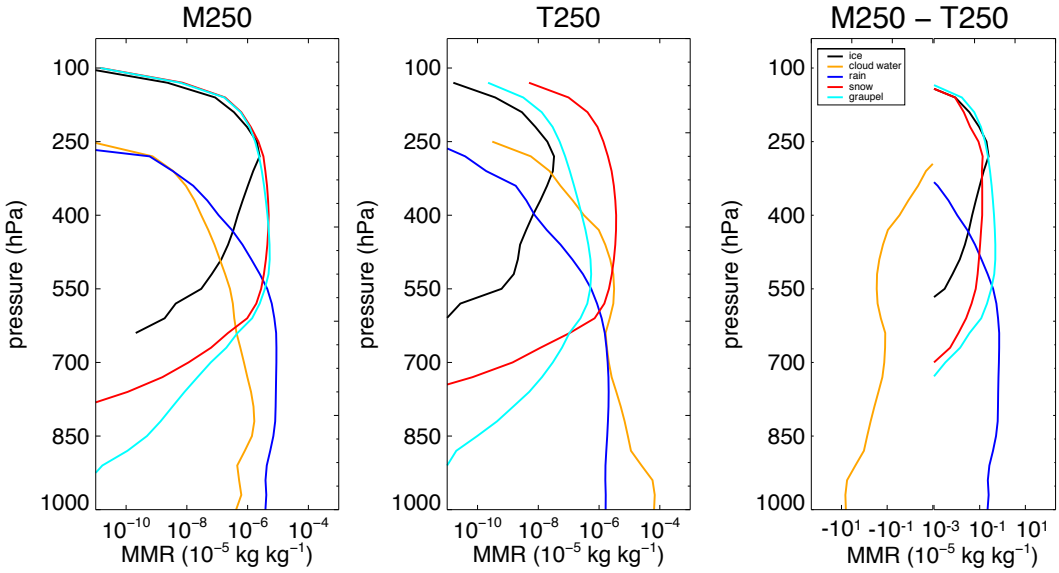

Figure R4: *Congo case: Domain-mean vertical profiles of hydrometeor mass mixing ratios (MMR) averaged over the period 1 – 10 August 2007. (a) CONGO-M250, (b) CONGO-T250 and (c) the difference in the domain-mean hydrometeor mixing ratio profiles (CONGO-M250 minus CONGO-T250). Note the logarithmic scale used on the*

horizontal axis in (a) and (b) to illustrate the large differences in the cloud water mass between the two simulations whilst also illustrating the differences in the frozen species. Note in (c) the diverging logarithmic 'difference' scale used on the horizontal axis, with 'negative' values extending from the centre to the left, and positive values extending from the centre to the right. The end of each of these axes is cut off at a value of 10^{-3}, however these axes tend towards each other towards zero.

14. P9, last paragraph and Figure 7, the huge increase of cloud water with the increase of CDNC with the Thompson scheme seems not reasonable. How about the change of precipitation?
We agree with the reviewer that the huge increase of cloud water with CDNC in the Thompson scheme in the Congo basin simulations is surprising. Our results show that this is accompanied by a reduction in precipitation (Figure 7, also noted in P10 L2, continued paragraph from last paragraph on P9). This is consistent with warm-phase precipitation suppression (Albrecht 1989). This is also consistent with our warm-phase RICO results, which show an increase in domain-averaged cloud mass and reduction in precipitation with CDNC in the Thompson scheme (Figure 12).

We suggest that the development of the warm cloud mass is likely due to the background meteorological conditions these simulations are performed in (see also our response to Reviewer 2's comment 21). We have shown that the autoconversion process is responsible for removing this cloud mass in the CONGO-MORR simulations. Our Figure 14 also shows that under increased CDNC, the threshold cloud water mass required for autoconversion to begin increases in the Thompson scheme. Therefore we suggest that increased levels of CDNC in the Thompson scheme in the Congo simulations even further suppress rain formation through autoconversion.

15. P. 10, L19-21: The sentence "we also see that the simulated hydrometeor classes differ between cases: the difference in the simulated hydrometeor classes in the idealised supercell configuration is different from the difference in the real-data Congo basin configuration" is not necessary. This is what it should be since they are different convective cloud types.
We have removed this sentence from our manuscript.

16. P11, first paragraph, the sentences in L5-6 and in L10-11 are repeated.
The first sentence refers to SUPER-MORR and CONGO-MORR, the second sentence to SUPER-THOM and CONGO-THOM. However, we have condensed these into a single sentence at the start of the paragraph (P14 L20):
"The SUPER-MORR and SUPER-THOM cases differs qualitatively from the CONGO-MORR and CONGO-THOM cases, respectively, both in the altitudes at which the response occurs and the sign of the response of some of the hydrometeors"

17. P11, first paragraph, the main point here should be about more significant aerosol impact on hydrometeor mass on the supercell case compared with the Congo case, not the different responses of hydrometeors between the CONGO case and the supercell case, since they should be expected for completely different cases. Many past studies have showed that aerosol impacts depend on dynamics and thermodynamics of convective clouds (e.g., Khain 2009; Fan et al. 2009).
We thought it necessary to place our results by first confirming that our results reproduce that hydrometeor response differs according to cloud type. However, we agree with Reviewer 2 that it would increase the clarity of our paper if we remove such discussion before presenting our results, and thank the Reviewer for suggesting that this can be taken as assumed knowledge. We also thank the reviewer for the suggestion of making our most important point here that the significance of aerosol impact differs between cases.

We have updated our text with these changes (P15 L1).

18. P11, last paragraph: the lack of appropriate sensitivity of bulk schemes to aerosols is mainly due to the limitation of bulk scheme parameterization in nucleation, diffusional growth, and sedimentation, etc, as detailed in Khain et al. 2015. The invigoration of updrafts can not be simulated since the saturation adjustment approach for diffusional growth of droplets limit such effects. Those aspects should be considered and discussed when interpreting the results on aerosol indirect effects here. Past studies showing the limitation of bulk scheme parameterizations in representing aerosol-cloud interactions need to be surveyed and discussed.
We agree with Reviewer 2 that saturation adjustment methods can prevent important physical processes from occurring in bulk schemes. We have now made extensive note in our introduction of past studies which show the limitation of bulk schemes in representing aerosol-cloud interactions (P2 L15 through P5 L16).

We also note that some bulk schemes produce convective invigoration effects. For example, Lebo 2014 found evidence of convective invigoration under increased aerosol loading in a bulk scheme under weak shear conditions (and suppressed convection under strong shear), similar to the findings of Fan 2009 who found the

same response in a bin scheme. Seifert 2006 also found higher overshooting tops and larger sizes of cumulonimbus in a weak shear environment with increased aerosol loading.

However, we emphasise that the main focus of this paper is not an investigation into aerosol and microphysical processes of convective invigoration (of which there is an extensive body of literature), but to highlight that the uncertainty due to choice of microphysics scheme can far exceed any simulated aerosol effects (even when using the WRF-SBM bin scheme, Figure S4 in the Supplement). Our Figure 10 is mainly used to illustrate that latent heating (and therefore dynamic impacts) differences due to the choice of microphysics scheme can equal those due to different levels of CDNC in a bulk scheme. (Unfortunately we cannot provide equivalent latent heating impacts for the WRF-SBM supercell simulation presented in our Supplement because we wrote the latent heating output into the Morrison and Thompson schemes for this study and have not had the chance to do this for the version of the HUJI SBM included in the public WRF release).

We agree with Reviewer 2 that our finding should be placed in the context of the literature which discusses the ability of bulk schemes to produce invigoration effects, and we have therefore included this discussion in our text.

19. P12, L5-7: Again physically it is supposed to be that for different types of convective cases. Hydrometeor differs and hydrometeor responses to CDNC are different as well.
This sentence was not supposed to convey that the hydrometeors and their response to CDNC differ in different convective cases (which, as Reviewer 2 has said, is supposed to be the case), but rather to highlight the source uncertainty due to the choice of microphysics scheme: response to CDNC varies in each scheme according to cloud / convection type (known), but the difference between the response of the two schemes to CDNC across types of convection is not systematic.

We strive to make our text as clear as possible, therefore we have rephrased our text to say 'the difference between the response of the two schemes to CDNC across types of convection is not systematic' (P16 L31-32).

20. P13, L23-25, reword the sentence. Not sure what you really want to say.
We have removed this sentence as we would need to re-run the simulations with autoconversion and accretion rates output in order to show this point.

21. P15, first paragraph, the authors showed the autoconversion process is not the significant process contributing to the large cloud mass at low –levels. Then the question is what process mainly contributes to it?
We have shown that the autoconversion process is responsible for the removal of the large cloud mass at low levels in the model configuration using the Morrison microphysics scheme. We also see that this low-level liquid cloud mass forms when we run the same simulation with the WRF-SBM implementation of the HUCM microphysics (Figures S2 and S3 in the Supplement), although to a lesser extent than in the Thompson simulations, and the warm cloud produced by the HUCM SBM produces rain. We therefore suggest that it is not the Thompson scheme per se which is responsible for producing the low-level cloud mass, but rather the meteorological conditions present in which these simulations are performed.

We now discuss this in our revised manuscript, P20 L10-16.

We provide here Figure R4 showing 3D isosurfaces of cloud water and ice mixing ratios for one snapshot in time of the WRF Congo simulations, 7 days into the simulation, at 01Z. Videos of such figures show firstly that the warm cloud mass forms mostly in the south-eastern region of the domain, over the ocean, and secondly that this cloud undergoes strong diurnal forcing.

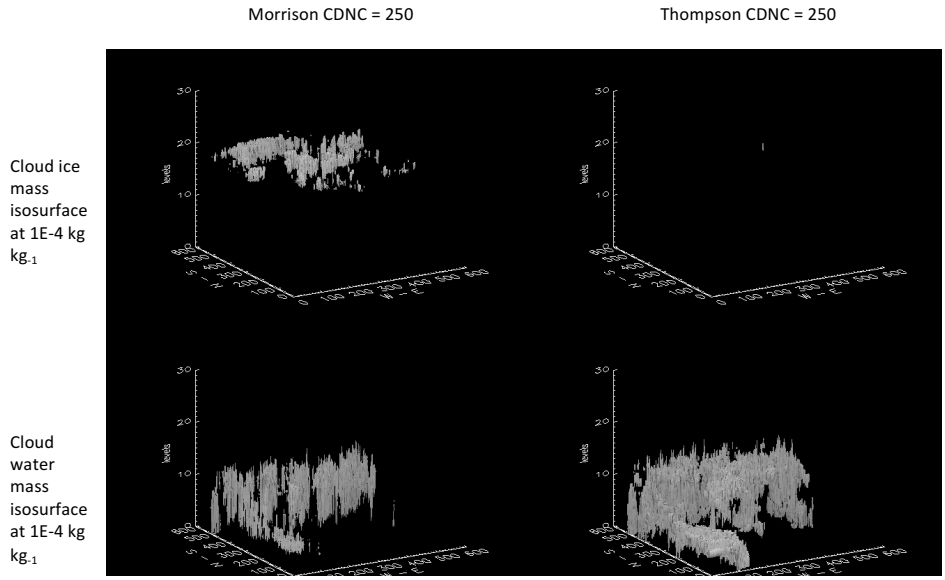

Figure R4: *Three-dimensional isosurfaces of cloud ice mass (top row) and cloud water mass (bottom row) for the M250 (left column) and T250 (right column) Congo case. The isosurface shown is the 1.E^{-4} kg kg^{-1} surface.*

However, regardless of the reasons for the development of the mass of warm cloud at low levels, the importance of our results is that under identical initial and lateral boundary meteorological conditions, the choice of microphysics representation on cloud development equals or exceeds that of cloud response to CDNC within each scheme.

22. P15, L19-20, again, the limitation of two-moment bulk schemes in representing aerosol impacts on microphysics processes should be discussed.
Bulk schemes have been shown to be limited in their ability to produce convective invigoration. Other studies using bulk and bin-bulk schemes have identified aerosol impacts on precipitation of up to about 15% (e.g. Kalina et al. 2014, Morrison 2012, Morrison 2011, Lebo et al. 2012, Lee & Feingold 2010, Lee & Feingold 2013, Lee 2011, van den Heever et al. 2006). Indeed, even studies using bin schemes have been shown to have little impact on total precipitation, although inducing a shift in rainfall rates (Fan et al. 2013).

We note that global modelling studies of aerosol indirect effects use bulk microphysics representations (e.g. Ghan et al. 2016, Zhang et al. 2016), and therefore our results have important implications for such studies.

We emphasise that our main result is to show that the variability due to, and within, schemes dominates any aerosol impacts on microphysics. Our results using the WRF-SBM in the idealised supercell case show that aerosol impacts in the bin scheme are of equal magnitude to those in the bulk schemes (Figure S4 in the Supplement).

We have included such a discussion in this section of the paper (P22 L24 through P23 L1) and also in the introduction (P2 L15 through P5 L16).

23. P17, L21-23, this sentence appears in a few places throughout the study, but the point can not be well justified even for aerosol indirect effects. First, you not know what the reality of aerosol look like in composition and spatial variability, many studies showed that aerosol spatial distribution could significant change storm location such as urban aerosols impact significantly on the precipitation in the downwind area of cities through aerosol indirect effects. Second, since two-moment bulk schemes even can not represent aerosol-cloud interaction processes physically, then how do you justify the aerosol impact here represent the upper limit?
We have removed these statements from our manuscript.

24. P18, L29, this is definitely not the first study to consider two and more cloud cases. A thorough literature search would give you those past studies.
We have removed this entire paragraph to make the conclusions more concise.

25. P18, L30-31, again, it has been a basic understanding that hydrometeors and their responses to CCN or CDNC vary with different cloud types and convective cases.
We agree with Reviewer 2 that this is basic understanding. As Reviewer 2 feels that this can be taken as assumed knowledge, we have increased the clarity of our paper by removing all such contextual discussion.

~~Can models robustly represent aerosol–convection interactions if their cloud~~ Uncertainty from choice of microphysics ~~is uncertain?~~scheme in convection-permitting models significantly exceeds aerosol effects

Bethan White[1], Edward Gryspeerdt[2], Philip Stier[1], Hugh Morrison[3], Gregory Thompson[3], and Zak Kipling[4]

[1]Atmospheric, Oceanic and Planetary Physics, University of Oxford, Oxford, UK
[2]Institute for Meteorology, Universität Leipzig, Leipzig, Germany
[3]National Center for Atmospheric Research, Boulder, Colorado
[4]European Centre for Medium-Range Weather Forecasts, Shinfield Park, Reading, UK

Correspondence to: Bethan White (bethan.white@physics.ox.ac.uk)

Abstract. This study investigates the hydrometeor development and response to cloud droplet number concentration (CDNC) perturbations in convection-permitting model configurations. We present results from a real-data simulation of deep convection in the Congo basin, an idealised supercell case, and a warm-rain large-eddy simulation (LES). In each case we compare two frequently used double-moment bulk microphysics schemes and investigate the response to CDNC perturbations. ~~In the Congo basin simulations both microphysics schemeshave large positive biases in surface precipitation, frequency of high radar reflectivities and frequency of cold cloud compared to observations~~We find that the variability among the two schemes, including the response to aerosol, differs widely between these cases. In all cases, differences in the simulated cloud morphology and precipitation are found to be significantly greater between the microphysics schemes than due to CDNC perturbations within each scheme. Further, we show that the response of the hydrometeors to CDNC perturbations ~~strongly differs~~ differs strongly not just between microphysics schemes but also ~~between different~~ that the inter-scheme variability differs between cases of convection. Sensitivity tests show that the representation of autoconversion is the dominant factor that drives differences in rain production between the microphysics schemes in the idealised precipitating shallow cumulus case and in a sub-region of the Congo basin simulations dominated by liquid-phase processes. In this region, rain mass is also shown to be relatively insensitive to the radiative effects of an overlying layer of ice-phase cloud. The conversion of cloud ice to snow is the process responsible for differences in cold cloud bias between the schemes in the Congo. In the idealised supercell case, thermodynamic impacts on the storm system using different microphysics parameterisations can equal those due to aerosol effects. These results highlight the large uncertainty in cloud and precipitation responses to aerosol in convection-permitting simulations and have important implications not just for ~~modelling~~ process studies of aerosol–convection interaction but also for global modelling studies of aerosol indirect effects. These results indicate the continuing need for tighter observational constraints of cloud processes and response to aerosol in a range of meteorological regimes.

1 Introduction

Deep convection has a significant influence on the state of the atmosphere and climate through shortwave and longwave radiative interactions, heat transfer through the release of latent heat, global heat redistribution, and plays an important part in the hydrological cycle through the conversion of water vapour to precipitation. ~~Aerosols~~ One major way that aerosols can influence the properties of deep convection is through their effect on cloud microphysics. By acting as cloud condensation nuclei (CCN), increased aerosol loading can lead to an increase in cloud droplet number concentration (CDNC) and subsequent reduction in cloud droplet size, which in turn has been hypothesised to suppress warm-phase precipitation (Albrecht, 1989). Some theoretical (e.g. Rosenfeld et al., 2008; Stevens and Feingold, 2009) and cloud (or cloud-system) resolving modelling studies (e.g. Fan et al., 2007b; Tao et al., 2007; Lebo and Seinfeld, 2011, amongst many others) have suggested that under certain conditions, precipitation suppression in the liquid phase may lead to an invigoration of deep convection and subsequent enhancement of convective precipitation. The detection of positive correlations between satellite-observed aerosol optical depth (AOD) and precipitation or convective cloud properties (e.g. Koren et al., 2005; Gryspeerdt et al., 2014) might suggest observational evidence of convective invigoration by aerosols. However, factors such as meteorological covariation and retrieval errors may contribute to or even dominate such correlations (Zhang et al., 2005; Mauger and Norris, 2007; Chand et al., 2012; Gryspeerdt et al., 2014). Complex process interactions in ice and mixed-phase microphysics, along with coupling to surface and radiative feedbacks and dynamics over a range of spatiotemporal scales, means that understanding and quantifying aerosol impacts on deep convection remains a significant challenge (e.g. Noppel et al., 2010; Seifert et al., 2012; Tao et al., 2012).

Representing cloud microphysical processes, which occur on length scales of microns to millimetres, has always been a significant challenge for atmospheric models. Even in cloud-resolving models, horizontal grid lengths tend to be on the order of kilometres to a few hundred metres at best, and so it is impossible for such models to explicitly simulate microphysical processes. There is a long history of microphysical parameterisation (see Khain et al., 2015, for a comprehensive review), and microphysics schemes today tend to fall into one of two categories: bin models, in which the size distribution of each hydrometeor class is explicitly calculated (e.g. Feingold et al., 1994; Stevens et al., 1996; Khain et al., 2004), and bulk models, in which a size distribution function typically is used to represent each hydrometeor class and one (or several) moments of the size distribution function are calculated explicitly (e.g. Kessler, 1969; Lin et al., 1983; Rutledge and Hobbs, 1983; Thompson et al., 2004; Morrison et al., 2005; Thompson et al., 2008, amongst many others). Bulk models are therefore very computationally efficient compared to bin models (often by at least two orders of magnitude, Jiang et al., 2000), and are used as standard in many atmospheric modelling systems today. Although certain aspects of cloud processes and aerosol indirect effects cannot be reproduced well in bulk schemes (see Khain et al., 2015, for a detailed analysis), there nevertheless remains a trade-off between how completely the hydrometeor size sprectra are represented and the physical domain size that can then be used in a simulation. For most applications, full bin microphysics (which can even resolve the autoconversion process of cloud water to rain) are only feasible using small domains and idealised simulations, which then cannot represent the dynamical feedbacks that can occur on larger domains (a notable exception, proving the cost of such simulations, are the multiple month-long case-study simulations using bin microph

Thus, studies using bulk and bin microphysics representations provide differently imperfect and thus complementary information. Indeed, bulk schemes remain as standard in global models, and there successful studies of aerosol indirect effects in global models have been performed using bulk microphysics (e.g. Zhang et al., 2016; Ghan et al., 2016).

Whilst early bulk microphysics schemes were single moment only ~~,~~ (predicting only the k=1 moment of the particle size distribution equation, mass), a significant development has been predicting ~~the second moment~~ two moments of the size distribution ~~, usually number concentration~~equation (k=0, number concentration, and k=1, mass) (e.g. Meyers et al., 1997; Thompson et al., 2004; Morrison et al., 2005; Thompson et al., 2008), which has been shown to have improved results compared to single-moment schemes (e.g. Lynn and Khain, 2007; Morrison and Grabowski, 2007; Morrison et al., 2009; Kumjian and Ryzhkov, 2012; Indeed, although not widely used at present, three-moment schemes have been shown to further improve representations of large hail (Milbrandt and Yau, 2006; Loftus and Cotton, 2014) and precipitation reflectivities (Kumjian and Ryzhkov, 2012).

However, bulk schemes make a priori assumptions about the shape of the particle size distributions (usually approximated by exponential or gamma distributions, and more rarely by lognormal functions), whereas bin schemes calculate particle size distributions by solving explicit microphysical equations and make no a priori assumption about the particle size distribution shapes. This can lead to significant differences in the cloud and precipitation simulated by bin versus bulk schemes. For example, bulk schemes have been shown to underestimate areas of weak and stratiform rain in an MCS compared to a bin scheme which performed better against observations (Lynn et al., 2005a, b), and Li et al. (2009a, b) showed that a one-moment bulk scheme was shown to be worse at partitioning rain into stratiform and convective components in a continental squall line compared to a bin scheme (although many studies have showed that two-moment schemes are a significant improvement on single-moment schemes, Lynn and Khain (e.g. 2007); Morrison and Grabowski (e.g. 2007); Morrison et al. (e.g. 2009); Kumjian and Ryzh Lynn and Khain (2007) found that, while all schemes overestimated maximum rain rates in a simulated MCS, all bulk schemes tested overpredicted average and maximum rain rates by a factor of 2 to 3, while bin schemes overestimated maximum rain rates by about 20%. In idealised supercell simulations, Khain and Lynn (2009) found that the Thompson et al. (2004) double-moment bulk scheme produced twice as much accumulated surface rain than a bin scheme, while Lebo et al. (2012) found that the Morrison et al. (2005) bulk scheme also produced twice as much surface rain as the same bin scheme used by Khain and Lynn (2009) in simulations of the same supercell.

Seifert and Beheng (2006a) found that the most important factor in achieving agreement in concentrations and mass contents between bulk and bin schemes in simulations of continental and tropical maritime clouds was accurate representation of warm-phase autoconversion. Sensitivity tests of 4 different autoconversion parameterisations conducted by Fan et al. (2012a, b); Wang et al that errors in predicting cloud water content in bulk schemes could be attributed to the saturation adjustment used in the calculation of evaporation and condensation. Likewise, Saleeby and van den Heever (2013) also showed, using 4 different types of autoconversion scheme, that saturation adjustment was the leading order factor in discrepancies of prediction of cloud water content by bulk schemes, and (Khain et al., 2016) found that tropical cyclones showed weak sensitivity to aerosol

due to the use of saturation adjustment . In the ice-phase, Li et al. (2009a, b) found artificial spikes in heating rates from deposition and sublimation due to the saturation adjustment scheme. Bryan and Morrison (2012) found that even at very high resolution, convective cores in an idealized squall line simulation remained undiluted due to the saturation adjustment used in the bulk microphysics scheme. However, saturation adjustment alone is insufficient to explain all differences between bin and bulk schemes: in idealised supercell simulations using bulk microphysics both with saturation adjustment and without (where the scheme was modified to include an explicit representation of supersaturation predicted over each time step), Lebo et al. (2012) found that the use of saturation adjustment was able to explain differences between a bulk and bin scheme in the response of cold pool evolution and convective dynamics under polluted conditions, but was not sufficient to explain the large differences in the response of surface precipitation to aerosol loading.

Differences between bin and bulk schemes can often be traced to their different process representations. For example, some studies have found rain evaporation in bulk schemes to be too fast compared to bin schemes (Fan et al., 2012a, b; Wang et al., 2013; Li et al. bulk schemes have been found to have higher condensation and evaporation rates, but similar rates of freezing and melting, compared to bin schemes (Li et al., 2009a, b). Shipway and Hill (2012) compared rates of diffusional growth, collisions, sedimentation and surface precipitation in several bulk schemes against results from the Tel Aviv University bin scheme (Tzivion et al., 1987) and found that precipitation peaks in the bulk schemes were too sharp and too narrow compared to the bin scheme, whereas the bin scheme produced weaker precipitation covering an overall larger area than that in the bulk schemes. Morrison and Grabowski (2007) tested three different parameterisations of the coalescence process in the Morrison et al. (2005) bulk scheme against a bin scheme, under different aerosol loadings and in both warm stratocumulus and warm cumulus clouds, and found that for both the bulk and bin scheme, each representation of the coalescence process led to different averaged rain contents and mean raindrop diameters. Fan et al. (2013) showed that, because bulk schemes do not represent size-resolved ice particle fall speeds, they were unable compared to bin schemes to simulate the reduced fall velocities of ice and snow at upper levels from clean to polluted conditions in tropical, mid-latitude coastal and mid-latitude summertime inland continental deep convective clouds. Fan et al. (2013) also suggested that bulk schemes tended to artificially freeze large raindrops, due to the use of a fixed gamma distribution.

In some cases, tuning particular processes in bulk schemes has led to better agreement with bin schemes, e.g. tuning evaporation rates and fall velocities of graupel in single-moment bulk scheme simulations of a continental squall line (Li et al., 2009a, b). Similarly, although no active tuning was performed, Seifert and Beheng (2006a) found that precipitation rates and accumulated precipitation values were in close agreement between simulations of continental and tropical maritime clouds in high and low CCN conditions using a bin and bulk scheme, with agreement between the bulk and bin scheme even greater in the high CCN case as compared to the low CCN case.

Not only do bin and bulk schemes often produce different results in terms of cloud and precipitation, but Fan et al. (2012a) found that the use of fixed CCN in a bulk scheme led to opposite CCN effects on convection and heavy rain compared to CCN effects

when using a bin scheme. Similarly, Lebo and Seinfeld (2011) found an opposite response of accumulated surface rain to CCN in idealised supercell simulations using a bulk and bin scheme, and Khain and Lynn (2009) found a difference in the response of an idealised supercell to aerosol perturbations when a bin and bulk scheme was used, with the bulk scheme producing stronger updraughts and greater average precipitation than the bin scheme, and with the left-moving storm prevailing in the bulk simulation while the right-moving storm prevailed in the bin simulation. The differences were attributed to differences in the vertical velocities in the bin versus bulk schemes, which led to hydrometeors ascending to different altitudes with different directions of background flow.

Nevertheless, bulk schemes have shown sensitivity to aerosol. In simulations of tropical deep convection, Morrison and Grabowski (2011) an ice-phase response to aerosol in which cloud top heights and anvil ice mixing ratios increase under polluted conditions, due to increased freezing of larger numbers of cloud droplets and subsequent higher ice particle concentrations with smaller sizes and reduced fall speeds. Indeed, a similar mechanism was later confirmed in bin-scheme simulations by Fan et al. (2013), who performed month-long simulations of deep convection over the tropical western Pacific, southeastern China and the U.S southern Great Plains. Further, Kalina et al. (2014) found that, autoconversion of cloud water to rain decreased under polluted conditions and, subsequently, near-surface rain and hail particles increased in size due to enhanced collection of cloud droplets. In simulations of deep convection over Florida using a bin-emulating bulk scheme, van den Heever et al. (2006) found that updraught strengths increased and anvil areas became smaller but better organized and with increased condensate mixing ratios. Similarly, in simulations of summertime convection over Germany using a two-moment bulk scheme, Seifert et al. (2012) found a strong aerosol effect on cloud properties such as condensate amounts and glaciation.

Unlike liquid cloud and rain drops (well-described by spheres of constant density), ice particles have a wide range of densities and shapes, making the representation of ice-phase microphysics in parameterisations much more difficult than the liquid phase. ~~Until recently~~Traditionally, the approach in both bin (e.g. Khain et al., 2004) and bulk schemes (e.g. Meyers et al., 1997; Thompson et al., 2004; Morrison et al., 2005, etc.) was to partition ice particles into one of a fixed number of categories (e.g. cloud ice, snow, hail and graupel) each with its own specified density, shape distribution and physical parameters such as fall speeds. However, such partitioning oversimplifies the complex nature of ice-phase processes, requiring thresholds and parameters - often chosen on a relatively ad hoc basis - to determine the partitioning of ice particles into each category and for converting between categories. As such, it is unsurprising that simulations have been found to be highly sensitive to particle fall speeds and densities (e.g. McFarquhar et al., 2006), the description of dense precipitating ice as hail or graupel categories (e.g. Morrison and Milbrandt, 2011; Bryan and Morrison, 2012), and changes in thresholds or rates for converting between ice categories (e.g. Morrison and Grabowski, 2008). Differences in ice-phase microphysics in bulk schemes have been shown to affect cloud biases especially at upper levels (Cintineo et al., 2014) and to affect ice–cloud–radiation feedbacks, with impacts on tropospheric stability, triggering of deep convection, and surface precipitation (Hong et al., 2009). Such limitations have led to the development in more recent years of new representations of ice microphysics in bulk schemes, such as approaches which separately prognose ice mass mixing ratios grown by riming and vapour deposition (Morrison and Grabowski, 2008),

where ice particle habit evolution is predicted by prognosing mixing ratios of ice crystal axes (Harrington et al., 2013), and where ice-phase particles are represented by several physical properties that evolve freely in time and space (Morrison and Milbrandt, 2015). Although these developments are relatively new, they have already been shown to improve simulations of observed squall lines and orographic precipitation when compared to traditional two-moment bulk schemes (Morrison et al., 2015a).

Evaluations of microphysics schemes frequently involve comparison against observations of a real precipitation event (e.g. Morrison and Pinto, 2005). Often, multiple microphysics schemes are compared against each other and against observations (e.g. Morrison and Pinto, 2006; Gallus Jr. and Pfeifer, 2008; Rajeevan et al., 2010; Jankov et al., 2011). Another common approach is to evaluate a single microphysics scheme against observations and then use different aerosol concentrations in the model to test the sensitivity of the observed storm to aerosol processes (e.g. van den Heever et al., 2006; Seifert et al., 2012). However, studies of different convective events in different regions, using different models with different microphysics schemes, often produce conflicting results on the nature of the storm repsonse to aerosol. Mesoscale studies of Florida convection found that cloud water mass, updraught strength and surface precipitation tend to increase with increased aerosol concentration, while anvil areas decreased but contain greater condensate mass (van den Heever et al., 2006), whereas studies of summertime convective precipitation in Germany found that increased aerosol concentrations had a strong effect on cloud microphysical (and therefore radiative) properties but that the combined effects of microphysical and dynamical processes resulted in relatively little effect on surface precipitation (Seifert et al., 2012), similar to the findings of Thompson and Eidhammer (2014) in idealised and continental-scale simulations.

Detailed process modelling studies of aerosol–convection interactions often focus on the sensitivity of a single idealised model configuration (without large-scale meteorology or surface and radiative interactions) to perturbations, using either CCN spectra (e.g. Seifert and Beheng, 2006b; Morrison and Grabowski, 2011) or CDNC values (e.g. Thompson et al., 2004; Morrison, 2012) as a proxy variable to test the sensitivity of the microphysics to aerosol. Many types of idealised models are used, ranging from flow over a 2D mountain (e.g. Thompson et al., 2004), 2D cloud-system resolving studies of interacting convective clouds (e.g. Morrison and Grabowski, 2011), to 3D simulations of idealised supercell storms (e.g. Khain and Lynn, 2009; Lebo and Seinfeld, 2011; Morrison, 2012; Lebo et al., 2012). With such a wide range of model configurations, convective and large-scale environments, microphysics parameterisations (bin and bulk models are both frequently used in idealised studies of aerosol–convection interactions) and proxy variables used to represent aerosol processes, it is perhaps not surprising that a consistent response of idealised convection to aerosol has not been seen and indeed, due to environment and regime-dependence, may not exist. Idealised flow over a 2D mountain using CDNC values to represent aerosol amounts showed that cloud water content increased with CDNC, and drizzle content decreased (Thompson et al., 2004), while a similar study using an idealised supercell configuration found that differences in the accumulated surface precipitation and convective mass flux between polluted and pristine values of CDNC were very small (Morrison, 2012). In studies using modified CCN spectra to represent different levels of aerosol in a two-moment scheme, 2D ensemble simulations of interacting convective clouds have

found that although cloud top heights and anvil ice increase under polluted conditions, convection actually weakens slightly compared to pristine conditions (Morrison and Grabowski, 2011). However, similar 3D simulations also using a two-moment microphysics scheme have shown that for isolated convective cells, increased aerosol leads to reduced total precipitation and updraught velocity, while for multicell systems it leads to increased secondary convection, total precipitation and updraught velocities, whilst supercell systems are relatively insensitive to aerosol (Seifert and Beheng, 2006b). Additionally, environmental wind shear has been shown to have a role in determining the response of convective systems to aerosol, with increased aerosol loading invigorating convection under weak shear conditions and suppressing convection under strong shear in simulations performed with both bin (Fan et al., 2009) and bulk (Lebo and Morrison, 2014) microphysics schemes.

~~Whilst previous studies have focused either on the response to CCN or CDNC perturbations of a particular idealised (e.g. Thompson et al., 2004; Seifert and Beheng, 2006b; Khain and Lynn, 2009; Lebo and Seinfeld, 2011; Morrison and Grabowski, 2011 or real-data (e.g. Morrison and Pinto, 2005; van den Heever et al., 2006; Seifert et al., 2012) model configuration, or the sensitivity of a particular precipitation event to different microphysics~~ The focus of this work is to show within a single modelling framework that uncertainty on cloud impacts through choice of microphysics scheme can far exceed any aerosol effect seen within a single scheme, and that this is a consistent finding across different types of convection in different environments and types of simulation (all of which are known to impact the effect of aerosol loading on cloud development, e.g. Altaratz et al., 2014). Although we use two bulk microphysics schemes to show this, there is a body of literature which identifies signals of aerosol impact on cloud in bulk schemes (e.g. Morrison and Grabowski, 2011; Morrison, 2012; Lebo et al., 2012; Kalina et al., 2014), albeit not always convective invigoration (see especially Lebo et al., 2012), and in bin-emulating bulk schemes (e.g. van den Heever et al., 2 Nevertheless, using a two-moment bulk scheme to simulate a single cumulonimbus in an environment characterised by high CAPE and low wind shear, Seifert and Beheng (2006a) found higher overshooting tops and larger sizes with increased aerosol loading, indicating that in some environments bulk schemes are able to produce invigoration effects. In some cases, aerosol effects may be relatively small (less than 15%, e.g. Morrison and Grabowski, 2011). However, while some argue (fairly) that this at least in part is due to the limitations of bulk schemes ~~(e.g. Morrison and Pinto, 2006; Gallus Jr. and Pfeifer, 2008; Rajeevan et al., 201 fewer studies have investigated the response of different microphysics schemes~~ to ~~perturbations in prescribed cloud parameters. Li et al. (2015) compared the response of two bulk microphysics schemes to two different CDNC values, but their study was limited to warm phase shallow convection. In simulations performed with bin microphysics , aerosols have been been shown to increase CDNC and reduce precipitation over eastern China (?) and to invigorate convection and suppress surface precipitation in idealised supercell cases (Khain and Lynn, 2009; Lebo et al., 2012), whilst equivalent simulations performed with bulk microphysicsresulted in little or no response to aerosol (Khain and Lynn, 2009; Lebo et al., 2012; ?).~~ fully represent aerosol-cloud interactions (such as saturation adjustment, Lebo et al., 2012), others argue that this is consistent with the concept of clouds as a buffered system hypothesized by Stevens and Feingold (2009). Month-long simulations approaching the climatological scale using bin microphysics performed by Fan et al. (2013) also showed aerosol impacts on precipitation on the order of a few %, however, those authors showed a significant aerosol impact on rain rates, rather than total rain amount, observing a shift towards heavier rain rates and fewer light rain rates under polluted conditions in two regions (a tropical environment and

midlatitude coastal environment), although the response in a midlatitude inland summertime continental environment varied temporally over the simulation. Similarly to the environmental-dependence found by Fan et al. (2013), Kalina et al. (2014) showed that even in an idealised simulation of a supercell using open boundaries and bulk microphysics, the relative humidity and shear used in the initial profile had an impact on the aerosol effects observed in the simulation.

~~In this work we investigate the reponse of different bulk microphysics schemes to idealised aerosol perturbations, but unlike previous studies we further compare the response across several different cases of convection.~~ We perform high-resolution convection-permitting simulations with the Weather Research and Forecast (WRF) model in three configurations: a real-data simulation of deep convection in the Congo basin, an idealised supercell case, and a shallow convection large-eddy simulation (LES). In each case we compare hydrometeor development in two commonly used double-moment bulk schemes and investigate the response of each model configuration to CDNC perturbations. Our focus is not to provide a detailed process study of aerosol effects on convection per se (to do so in the context of multiple model configurations is beyond the scope of this paper), but rather to explore and identify uncertainty in the cloud and precipitation response to CDNC perturbations across a range of model configurations. We acknowledge that, due to a lack of fully coupled aerosol-cloud processes ~~(e.g. droplet activation, wet deposition and buffering processes, Stevens and Feingold, 2009; Lee and Feingold, 2010; Seifert et al., 2012)~~ the magnitude of response of bulk microphysics schemes to CDNC perturbations may ~~exceed~~ differ from that in schemes that explicitly treat cloud processing of aerosol. Our goal therefore is to highlight the large uncertainty in cloud and precipitation responses to perturbations of CDNC in convection-permitting models, even between multiple configurations of the same widely used model.

2 Experimental design

We use the Advanced Research WRF version 3 (Skamarock et al., 2008) in three different configurations: a real-data simulation of deep convection over the Congo basin, an idealised supercell simulation, and a warm-rain shallow cumulus LES simulation. WRF is a nonhydrostatic, compressible, 3D atmospheric model. We use version 3.5 of WRF in the Congo basin and the idealised supercell simulations, but version 3.3.1 was utilised for the warm-rain LES simulation because the LES packages were only available for this version of the model at this time (Yamaguchi and Feingold, 2012). In order to keep the simulations as consistent with each other as possible, we therefore implement the versions of the microphysics schemes from WRF version 3.5 into version 3.3.1 of the model for the LES simulations. Each set of simulations is performed using two microphysics parameterisations, at three different prescribed CDNC values, resulting in a total of six simulations for each model configuration. The model configurations used in this study are summarised in Table 1.

2.1 Microphysics parameterisations

This study is presented as an indication of the uncertainty that can arise from choice of microphysics scheme alone, and thus we restrict our comparison to two double-moment bulk microphysics schemes rather than diversify into a comparison of bin schemes against bulk schemes. The literature surveyed in Section 1 indicates the wide range of differences that may be expected when comparing bulk against bin schemes. A significant body of work has shown that two-moment bulk microphysics schemes generally represent cloud and precipitation characteristics more realistically than single-moment schemes (most recently Morrison et al., 2009; Wu and Petty, 2010; Weverberg et al., 2013, 2014; Igel et al., 2015), and thus our study is restricted to the comparison of two five-class, double-moment schemes commonly used in WRF and shown by Cintineo et al. (2014) to perform well against satellite observations of cloud in North America: that described by Morrison et al. (2005, 2009); Morrison and Milbrandt (2011) (hereafter Morrison, or abbreviated to MORR), and that described by Thompson et al. (2004, 2008) (hereafter Thompson, or THOM). Both schemes are two-moment in rain and ice (prognostic mass and number), while the Morrison scheme is also two-moment in snow and graupel. Both are single moment in cloud water: mass is the only prognostic liquid cloud variable, and CDNC is prescribed at a given value. Following the method used in many previous studies including ~~those of Khain and Lynn (2009) and Morrison (2012) ,~~ that of Morrison (2012) we prescribe CDNC values (in this study, at 100, 250 and 2500 cm^{-3}) as a proxy for CCN varying under conditions ranging from clean to highly polluted. The list of microphysics configurations tested and the abbreviations used to describe them are summarised in Table 2.

2.2 Model configurations

The real-data Congo simulations use a model domain covering a 2100 km × 2100 km region over the Congo Basin (Figure 1), chosen due to the high frequency of isolated deep convective systems occurring in the region and also due to the presence of strong sources of biomass burning aerosol. The model initial and boundary conditions were generated from ERA-Interim reanalysis (Dee et al., 2011), starting at 00:00 UTC on 1 August 2007. The simulation start date was chosen to coincide with the onset of the seasonal peak in precipitation (Washington et al., 2013) and the simulation was integrated for 10 days (with a timestep of 12 s) in order to identify the nature of the convection and its repsonse to CDNC perturbations over timescales greater than that of the lifecycle of any individual convective system. We use a horizontal grid length of 4 km and 30 vertical levels with the standard WRF stretched vertical grid. This gives a vertical grid spacing of about 100 m in the lower levels, with grid spacing increasing towards the upper levels. Although 30 vertical levels may seem relatively coarse, it has been shown in a previous study to be sufficient to reproduce observed cloud morphology and resolve the vertical structure of aerosol and precipitation and their interactions in this region (Gryspeerdt et al., 2015). Longwave and shortwave radiation in the simulations are parameterised by the RRTM (Mlawer et al., 1997) and Goddard (Chou and Suarez, 1994) schemes, respectively. Other physics parameterisations (other than the microphysics schemes previously discussed) are the MM5 Monin-Obukhov similarity surface layer scheme available in WRF (which uses stability functions and surface fluxes from Dyer and Hicks, 1970; Paulson, 1970; Webb, 1970; Beljaars, 1994), the NOAH land surface model (Ek and Mahrt, 1991) and the YSU boundary layer scheme (Hong et al., 2006), also shown by Cintineo et al. (2014) to perform well.

The idealised supercell setup follows the standard 3D idealised supercell case available as part of the WRF modelling system. Boundary conditions are open on all lateral boundaries, and the model top and surface are free-slip. For consistency with the Congo basin simulations, we use a horizontal grid length of 4 km. The model domain is 1600 km × 1600 km in the horizontal and, for consistency with the Congo simulations, also uses 30 vertical levels with a model lid at 20 km. A Rayleigh damper with damping coefficient of 0.003 s^{-1} is applied in the top 5 km of the model to prevent spurious wave reflection off the model top. Following the setup commonly used in idealised supercell studies (e.g. Morrison, 2012), surface energy fluxes, surface drag, Coriolis acceleration and radiative transfer are neglected for simplicity, and the subgrid-scale horizontal and vertical mixing is calculated with a prognostic turbulent kinetic energy scheme (Skamarock et al., 2008). The model is initialized as in the idealised quarter-circle supercell test case available in WRF, using the analytic sounding of Weisman and Klemp (1982, 1984) and the quartercircle supercell hodograph of Weisman and Rotunno (2000) with the shear extended to a height of 7 km. Convection is triggered using a thermal perturbation in the centre of the domain, with maximum perturbation potential temperature of 3 K centred at a height of 1.5 km and with horizontal and vertical radii of 10 km and 1.5 km, respectively. All simulations are integrated for 2 h with a timestep of 12 s (the same timestep used in the Congo simulations).

The warm-rain shallow cumulus setup deviates from the other simulations in that it follows the LES intercomparison guidelines for the Precipitating Shallow Cumulus Case 1 (van Zanten et al., 2011) of the Rain in Shallow Cumulus Over the Ocean (RICO, Rauber et al., 2007) project and uses the RICO WRF LES package provided by Yamaguchi and Feingold (2012). The model domain is 12.8 km × 12.8 km × 4 km with a horizontal grid spacing of 100 m and uses 100 vertical levels, implying a vertical grid spacing of about 40 m. The lateral boundary conditions are doubly periodic. As in the idealised supercell simulations, surface energy fluxes, surface drag, Coriolis acceleration and radiative transfer are neglected for simplicity, and the subgrid-scale horizontal and vertical mixing is calculated with a prognostic TKE scheme. The surface conditions, wind and thermodynamic profiles, large-scale forcings and large-scale radiation, geostrophic wind, initial perturbations and translation velocity are prescribed following the RICO case guidelines (van Zanten et al., 2011). For consistency, we prescribe cloud droplet number concentrations at 100, 250 and 2500 cm^{-3} following the other simulations in our study, instead of the 70 cm^{-3} suggested for the standard RICO case. However, we also perform an extra simulation at 50 cm^{-3}. The simulations are integrated for 24 h with a timestep of 1 s.

3 Results

3.1 WRF Congo basin~~: real-data simulations~~

Maps of simulated outgoing longwave radiation (OLR) and surface precipitation at 0700 UTC on 7 August 2007 (7 days into the simulation) indicate that the cloud morphological and precipitation differences for different microphysics schemes are much greater than the cloud and precipitation response within each scheme to different CDNC values (Figure 1). In the CONGO-MORR simulations, low OLR values (indicating cold, high cloud) are distributed across the domain. Precipitation at

this time occurs only in cloud north of 3° S, but there is a large band of non-precipitating cold cloud across the south of the domain. There is little discernable response of the morphology of the OLR and precipitation in the CONGO-MORR simulations to different CDNC values (Figs. 1a, 1b and 1c). In comparison, cold cloud in the CONGO-THOM simulations ocurrs mostly north of 3° S (Figs. 1d, 1e and 1f). Less cloud forms in CONGO-THOM compared to CONGO-MORR, and the cloud generally has greater OLR values than that in CONGO-MORR. Some non-precipitating cloud occurs south of 3° S in the CONGO-THOM simulations, but the band is significantly weaker and warmer than in CONGO-MORR. The differences at this snapshot are representative of differences that persist throughout the simulation. Frequency distributions of OLR over the entire 10-day simulation period show that CONGO-MORR has a much higher frequency of occurrence of colder, higher cloud (values about 120 W m^2) than CONGO-THOM (which increases in frequency slightly with increased CDNC), while CONGO-THOM has a much higher frequency of occurrence of warmer cloud (values about 270 W m^2) than CONGO-MORR (Figure 2a). When compared to observations of OLR from the Geostationary Earth Radiation Budget (GERB, Harries et al., 2005) over the same region and period, CONGO-THOM represents warm cloud more consistently with GERB than CONGO-MORR, despite overpredicting colder cloud somewhat, while CONGO-MORR overpredicts higher cloud and underpredicts warm cloud compared to the observations (Figure 2a). However, despite a poorer prediction of cloud radiative properties, CONGO-MORR predicts surface precipitation better than CONGO-THOM when compared to observations from the Tropical Rainfall Measuring Mission (TRMM, Huffman et al., 2007) merged product. Both schemes significantly overpredict surface precipitation compared to observations from the TRMM 3B42 product (although the spatial patterns of precipitation are reasonably similar), however total accumulated surface precipitation over the 10-day simulation period is much greater in CONGO-THOM than CONGO-MORR (Figure 3). Further differences are seen when the distributions of precipitation rates are compared, with CONGO-THOM overpredicting and CONGO-MORR underpredicting the occurrence of low precipitation rates compared to TRMM, CONGO-MORR overpredicting and CONGO-THOM underpredicting moderate rates, and CONGO-THOM overpredicting the frequency of occurrence of very high precipitation rates (Figure 2b). That CONGO-MORR overpredicts the frequency of moderate rain rates and CONGO-THOM overpredicts the frequency of very high rain rates likely explains why both schemes overpredict total accumulated surface rain compared to the observations. Additionally, the overprediction of the frequency of very high precipitation rates by CONGO-THOM is likely the reason that the total accumulated surface precipitation is much greater in this scheme than in CONGO-MORR (Figure 3a,b).

Further to the significant difference between the two schemes in their reproduction of cold cloud and precipitation rates, the updraught dynamics respond very differently to aerosol loading. Joint histograms of cloud top height in the convective updraughts and the radius of the updraughts show that the most significant dynamical difference between the simulations comes from choice of microphysics scheme: the Morrison scheme has a tendency towards higher frequencies of wider updraught radii with higher cloud tops than the Thompson scheme (Figure S1 in the Supplement). Under increased values of CDNC, convection in the CONGO-MORR simulation shifts towards wider cores and higher core tops for mid-sized cores (radius 11 to 22 km), whilst there is a reduction in the frequency of smaller cores of all core top heights (Figure 2c). Conversely, convection under polluted conditions in the CONGO-THOM simulation shows a reduced frequency of occurrence of the highest updraught

cloud tops for all updraught radii under polluted conditions, with an increased frequency of occurrence of small updraught radii with lower cloud tops (Figure 2d). Therefore, a consistent aerosol response is observed in CONGO-THOM, resulting in smaller and lower convective updraughts (i.e. weakened convection under polluted conditions). Interestingly, both of these effects contradict the findings of Morrison and Grabowski (2011), who found an ice-phase response to aerosol in which cloud top heights and anvil ice mixing ratios increase under polluted conditions due to increased freezing of larger numbers of cloud droplets and subsequent higher ice particle concentrations with smaller sizes and reduced fall speeds. However, we note that we consider different values of CDNC / CCN to Morrison and Grabowski (2011) and that responses may be nonmonotonic Kalina et al. (2014), and that we consider a different case of convection (indeed, our 10-day Congo simulation covers many convective lifecycles). We note that the response of the convective updraughts to aerosol loading in these two bulk schemes cannot be attributed to saturation adjustment alone (the suggested effects of which on updraught invigoration are detailed in Khain et al., 20 because both schemes use this method.

Not only does the simulated cloud and precipitation morphology differ significantly between microphysics schemes irrespective of the CDNC values used in the comparison, zonal-mean vertical sections of mass mixing ratios of the different hydrometeor classes show significant differences in the ~~hydrometero~~ hydrometeor classes (due to microphysics) between CONGO-MORR and CONGO-THOM (Figure 4). The most significant difference between the two microphysics schemes is that south of 3° S, CONGO-MORR produces a large amount of high ice cloud between 300 and 150 hPa (Figs. 4a, b, c). Analysis of these vertical sections at hourly intervals throughout the simulation in conjunction with hourly maps of OLR as in Figure 1 show that this upper-level ice is transported from the convective anvils in the north of the domain to the non-convective region in the south of the domain (not shown). In comparison, CONGO-THOM produces significantly less ice, with almost no ice visible at this contour value (Figs. 4d, e, f). However, all three CONGO-THOM simulations form a large amount of non-precipitating low-level (950 to 850 hPa) liquid cloud south of 3° S. The bands of cloud seen south of 3° S in Figure 1 are therefore high ice cloud in the CONGO-MORR simulations and low liquid cloud in the CONGO-THOM simulations, illustrating not only a cloud morphological difference between the microphysics schemes but also a significant difference in the simulated hydrometeor classes and in the vertical distribution of hydrometeors. Even in the convective precipitating region in the north of the domain, the simulated hydrometeor classes differ significantly between the microphysics configurations, with the CONGO-MORR simulations generating more ice and less liquid cloud (Figs. 4a, b, c) and the CONGO-THOM simulations producing less ice and more liquid cloud (Figs. 4d, e, f). Rain is confined to the convective region in the north in CONGO-THOM, while in CONGO-MORR it is also present at low levels in the non-convective southern region of the domain which is dominated by liquid cloud in CONGO-THOM. We explain the mechanisms behind these differences later, but here we highlight that it is clear from Figure 4 that the differences in the simulated hydrometeors between microphysics schemes are much greater than the differences due to different levels of CDNC.

Because the partitioning of water into liquid and ice phases in the full-physics model configuration appears to depend strongly on the microphysics scheme, vertical sections of reflectivity occurrences derived from model hydrometeor fields

passed through the Quickbeam radar simulator (Haynes et al., 2007) are compared against ~~an August reflectivity occurrence climatology~~ equivalent reflectivity occurrences from the CloudSat 2B-GEOPROF product (Marchand et al., 2008) (Figure 5). The histograms are derived from the reflectivity fields thresholded to include all values greater than -20 dBZ. ~~Note that the model data are from the 10-day simulation period only, sampled to the times nearest to each CloudSat overpass, whereas the satellite data show a mean of all overpasses that occur in August in the Congo basin domain over a 6 year period. With this limitation in mind, we use the satellite radar data for a qualitative comparison only. The satellite data show that the model produces the highest reflectivities in the~~ The largest reflectivity values produced by the model occur in the convective region in the north of the domain, where the ~~highest reflectivities are also observed~~ largest reflectivity values are detected by the satellite radar (Figure 5), also in agreement with the TRMM precipitation observations (Figure 3). However, both CONGO-MORR and CONGO-THOM have a large positive bias in reflectivity compared to the ~~observed climatology~~ observations (Figure 5), indicative of limitations in the ability of both bulk microphysics schemes to represent the observed vertical cloud structure in this geographic region over this time period. In general, CONGO-MORR has a much larger positive bias in reflectivity than CONGO-THOM (Figure 5). The CloudSat observations show a small frequency of occurrence of reflectivities detected at altitudes of 10 to 15 km in the south of the domain, which is well-represented by CONGO-THOM and indicates the overproduction of ice in CONGO-MORR (Figure 5).

Differences in the simulated hydrometeor classes between the schemes persist throughout the simulation and are illustrated by ~~domain-mean~~ mean profiles of hydrometeor mass mixing ratios (Fig. 6). ~~Most significantly , most of the~~ There is significantly more ice-phase condensate in the CONGO-M250 configuration ~~is partitioned into the ice phase~~ (Fig. 6a), whereas the CONGO-T250 profile is dominated by a large amount of liquid cloud mass between the near-surface and 750 hPa (Fig. 6b). The differences in the total cloud water mass between the schemes are very large: at 950 hPa (the altitude with the greatest liquid cloud mass in CONGO-T250, Figure 6), cloud water mass contents are about 140× greater in CONGO-T250. The liquid cloud mass is always greater in CONGO-T250 than CONGO-M250 (Fig. 6c), by several orders of magnitude at some levels, but despite this the liquid phase does not appear to drive differences in precipitation between the microphysics schemes: CONGO-M250 has about 4× more rain mass in the mid-levels and 2× more rain mass near the surface than CONGO-T250 (Figs. 6a and b). In the ice phase, CONGO-M250 has only slightly more snow mass than CONGO-T250 but up to 10× more graupel mass (Figs. 6a and b) and while ice is a significant hydrometeor at upper levels in CONGO-M250, CONGO-T250 has almost no cloud ice at all (Figs. 6a and b). We note that the magnitude of the difference due to choice of scheme is the same when a bin scheme is used (Figures S2 and S3 in the Supplement).

Mean profiles over all condensed points (i.e. representing the mean values of each hydrometeor type, but not accounting for changes in absolute quantities across the model domain) show that CONGO-T250 has consistently more cloud water through the depth of the mean cloud compared to CONGO-M250 (Figures 6a, b), while CONGO-M250 produces more rain (Fig. 6a). That rain production in CONGO-M250 occurs mostly through the depths of the atmosphere where cloud water persists suggests that a significant proportion of the rain may be produced though autoconversion in CONGO-M250, although

note that these mean cloud profiles are calculated over the entire domain and therefore incorporate both the deep convective region in the north and the warm-cloud region in the south, as seen in Fig. 4. Further, the two schemes show differences in the frozen hydrometeors, with the mean cloud in CONGO-M250 containing more graupel and less snow than CONGO-T250 (Fig. 6c). This may be an result of the use of distinct and different definitions of ice-phase hydrometeor categories in the two schemes, which have been shown to cause deficiencies in simulations of observed squall lines (Morrison and Milbrandt, 2015).

Not only does the partioning of ice amongst the hydrometeor classes differ between schemes, the response of the hydrometeors to CDNC perturbations also differs between schemes (Fig. 7). First note that the scale of the hydrometeor response to CDNC perturbations in the CONGO-MORR simulations is an order of magnitude smaller than the scale of the repsonse in the CONGO-THOM simulations. ~~Liquid~~ Over the entire domain, liquid cloud mass appears insensitive to CDNC perturbations in the CONGO-MORR configuration (Fig. 7a)~~.~~, although a reduction of mean-cloud liquid cloud mass under polluted conditions (Fig. 7c) indicates that there must be very few liquid cloud points in the CONGO-MORR simulation compared to other hydrometeor types, notably ice (Fig. 7a). Very weak decreases in domain-mean near-surface rain mass may be evident under polluted conditions in CONGO-MORR, but this difference is on the order of 10^{-8} kg kg^{-1} (Fig. 7a) ~~.~~A reduction in rain mass under polluted conditions is more evident in the mean rain profile (Fig. 7c), again indicating how few rainy points exist compared to other hydrometeor types in CONGO-MORR when considering the entire domain (Fig. 7a). Nearly all of the hydrometeor response in CONGO-MORR occurs in the ice phase processes: graupel mass decreases significantly under polluted conditions ~~, while ice and snow mass increase~~ (Fig. 7a,c), while ice mass increases at upper levels in both a domain-mean and ice-mean sense (Fig. 7a,c). In contrast, the hydrometeor reponse to CDNC perturbations in the CONGO-THOM configuration is an order of magnitude greater than in CONGO-MORR and the dominant hydrometeor response to CDNC perturbations in CONGO-THOM occurs in the liquid phase. Not only does the CONGO-THOM configuration generate a significant amount more liquid cloud than the CONGO-MORR configuration (Figure 6c), but the liquid cloud mass increases under polluted conditions by an order of magnitude more than any other hydrometeor response (Fig. 7b,d). Rain mass ~~decreases with increased CDNC~~ is relatively insensitive to increased CDNC in CONGO-THOM (Fig. 7b~~),while snow production appears to shift to lower levels~~ ,d). The significant difference between the response of the two schemes to perturbations in CDNC, with CONGO-MORR producing less liquid cloud and rain under polluted conditions ~~, with a decrease in snow mass between 375 and 200 hPa and an increase in snow mass of about the same amount between 600 and 400 hPa (Fig. 7b).~~ while CONGO-THOM produces more cloud water, indicates significant differences in the cloud processes represented by the two schemes in this meteorological regime.

3.2 WRF idealised supercell~~: ice phase processes~~

The results from the real-data Congo basin simulations indicate that the development of the simulated hydrometeor classes and the reponse of the hydrometeors to CDNC perturbations depend strongly on the choice of microphysics scheme. ~~A few~~ Although some previous studies have focused on the response of real-data case studies to both microphysics scheme and CDNC

response ~~(e.g. ?Fan et al., 2013; Li et al., 2015), but~~ (e.g. Fan et al., 2012a, 2013; Li et al., 2015), there is a much larger body of literature that investigates the repsonse of idealised supercell simulations to CDNC (or CCN) perturbations (e.g. Seifert and Beheng, 2006b; Khain and Lynn, 2009; Lebo and Seinfeld, 2011; Morrison, 2012). We therefore place our study in the wider context of the existing literature ~~, simultaneously allowing us to explore the case-dependence of the deep convective response to aerosol effects,~~ by investigating the reponse of a single isolated idealised supercell under both the MORR and THOM microphysics configurations to the same CDNC perturbations used in our Congo simulations, simultaneously allowing us to explore the case-dependence of the deep convective response to aerosol effects.

Figure 8 shows ~~domain-mean~~ mean hydrometeor profiles from the idealised supercell model configurations under 'moderately polluted' prescribed CDNC values of 250 cm^{-3}. As in the Congo basin case, it is clear that the simulated hydrometeor classes differ significantly between schemes. ~~However, we also see that the simulated hydrometeor classes differ between cases: the difference in the simulated hydrometeor classes in the idealised supercell configuration is different from the difference in the real-data Congo basin configuration (Figure 8 compared to Figure 6).~~ In contrast to the Congo basin configuration, both the SUPER-MORR and SUPER-THOM configurations show similar behaviour in the liquid phase, producing similar profiles of liquid cloud mass and rain mass in both a domain-mean and hydrometeor class-mean sense (Figures 8a,d and 8b,e), and instead the most significant differences occur in the ice phase. Graupel dominates as the frozen precipitating hydrometeor in the SUPER-M250 configuration, amounting to about 4× the snow and ice masses at their peak amounts (Figure 8a,d). In contrast, snow is the dominant frozen precipitating hydrometeor in the SUPER-T250 configuration, amounting to about 1.5× the graupel mass at their peak amounts and virtually no ice present (Figure 8b,e). Although there is very little difference between the SUPER-MORR and SUPER-THOM configurations in the liquid phase (except for the SUPER-MORR configuration producing about 2×10^{-7} kg kg^{-1} less domain-mean rain mass at the surface than SUPER-THOM, Fig. 8c), the SUPER-MORR configuration forms significantly more ice, more graupel and less snow than SUPER-THOM (highlighting that the partitioning of ice-phase hydrometeors into categories is very different, by design, in different microphysics schemes), and greater total quantities of frozen hydrometeors are present between 600 and about 150 hPa in SUPER-MORR compared to SUPER-THOM (Fig. 8c,f). This is a significant difference from the Congo real-data configuration, where the dominant contribution to the difference between the CONGO-MORR and CONGO-THOM configurations came from the liquid cloud (Figure 6c).

~~In the real-data Congo basin configuration the response of the hydrometeors to CDNC perturbations was shown to differ between schemes~~ There is a more significant aerosol impact on hydrometeor mass in the supercell case than in the Congo case for both microphysics schemes, with mean responses over each hydrometeor type an order of magnitude greater in the supercell case (Fig. 7 ~~).This also occurs for the idealised, isolated supercell configuration (Figure~~compared to Fig. 9). ~~However, the hydrometeor~~ Although many past studies have shown that aerosol impacts depend on cloud dynamics and thermodynamics (e.g. Khain and Lynn, 2009; Fan et al., 2009), we note that not only do the individual schemes respond differently to CDNC in different cases of convection (as expected) but that the way the schemes differ from each other in their response to CDNC ~~perturbations also differs between the two cases~~is significantly different in the supercell case compared to the Congo case.

The SUPER-MORR ~~case~~ and SUPER-THOM cases differs qualitatively from the CONGO-MORR ~~case~~ and CONGO-THOM cases, respectively, both in the altitudes at which the response occurs ~~,~~ and the sign of the response of some of the hydrometeors. In the SUPER-MORR configuration, cloud water mass increases under polluted conditions, and rain mass is suppressed at mid-levels (between 600 and 450 hPa) but shows negligible response at the surface (Fig. 9a,c). In the ice phase, cloud ice increases under polluted conditions in SUPER-MORR, while graupel and snow decrease (Fig. 9a,c). Similarly, the hydrometeor response of the SUPER-THOM case to CDNC perturbations also differs in sign and in altitude to CONGO-THOM. In SUPER-THOM, cloud water mass increases and rain mass decreases under polluted conditions (Fig.9b,d), but unlike SUPER-MORR the decrease in rain is evident at the surface. Graupel mass decreases under polluted conditions in SUPER-THOM, similarly to SUPER-MORR but occurring over a much larger range of heights (Fig.9b,d), but unlike CONGO-THOM, which shows very little response to polluted conditions (Fig.7c). ~~The dominant hydrometeor~~ Interestingly, this is in contrast to Khain and Lynn (2009), who found an increase in graupel mass with increased CDNC in the Thompson scheme. However, their study was of 2D idealised squall line simulations, and considered CDNC values of 100, 500 and 100 drops per cm^{-3}. The dominant domain-mean response to increased CDNC perturbations in SUPER-THOM is an increase in snow mass between 550 and 150 hPa (Fig.9b)~~.~~, which likely comes from lofting of an increased mass of cloud water (Fig.9d). This is in contrast both to SUPER-MORR, where the dominant hydrometeor reponse occurred in the ice class (Fig.9a) despite and almost equal increase in lofted cloud water (Fig.9c), and to CONGO-THOM, where the dominant hydrometeor reponse occurred in the liquid cloud (Fig.7b). That both schemes show an increased lofting of cloud water under polluted conditions (Figs7c,d) but SUPER-MORR responds by generating more cloud ice (Figs7a,c) while SUPER-THOM shows an increase in snow (Figs7b,d) suggests differences in the processes that convert cloud ice to snow. This is explored later in Section 3.4. We emphasise that our main result shows that the variability due to microphysics scheme dominates any aerosol impacts on microphysics. Results using the WRF-SBM in the idealised supercell case show that aerosol impacts in the bin scheme are of equal magnitude to those in the bulk schemes (Figure S4 in the Supplement).

To further investigate the importance of the difference in microphysics representations and the difference in their response to CDNC perturbations, Figure 10 includes the domain-mean total latent heating (sum of the latent heating from individual microphysical processes) contributions for each of the idealised supercell configurations. It can be seen that the choice of microphysics scheme can result in thermodynamic differences in the supercell system equal in magnitude to those arising from CDNC perturbations: between 500 and 250 hPa, the latent heating rate in the SUPER-M2500 configuration is almost identical to that in the SUPER-T250 configuration (solid red and dashed blue lines, Figure 10a). Thus, the magnitude and sign of the difference in the latent heating rate between SUPER-M250 and SUPER-T250 (blue solid and dashed lines, Figure 10a) is the same as that between SUPER-M2500 and SUPER-M250 (red and blue solid lines), and likewise the magnitude and sign of the difference in the latent heating rate between SUPER-M2500 and SUPER-T2500 (red solid and dashed lines) is the same as that between SUPER-T2500 and SUPER-T250 (red and blue dashed lines). In general, the SUPER-THOM configuration has a much stronger thermodynamic response to CDNC perturbations than the SUPER-MORR configuration, with latent heating rates consistently stronger throughout the atmosphere (Figure 10b). Overall, there is little

evidence of convective invigoration (defined here as increases in upper-tropospheric heating, updraught strengths, cloud top height and surface precipitation) under increased CDNC values in either bulk microphysics scheme: although both schemes show increased latent heating in the upper troposphere and decreased heating at mid-levels under polluted conditions (Figure 10b), it has already been shown that there is no evidence of increased surface precipitation (Figure 9), and the upper tropospheric peak in latent heating can be seen to correspond to an increase in ice (SUPER-M250) or snow (SUPER-T250) at these levels (Figure 9). Neither is there any systematic or consistent evidence of increased mean updraught velocity in the convective cores (following the method of van den Heever et al., 2006; Lebo and Seinfeld, 2011) under polluted conditions (not shown). , or in increased cloud top heights of the convective cores (Figs. 2c,d). This may not be surprising, as it has been suggested that bulk microphysics schemes are unable by design to produce convective updraught invigoration effects due to limitations in their representation of nucleation, sedimentation, and the way in which saturation adjustment limits diffusional growth (detailed in Khain and Lynn, 2009). Indeed, Lebo and Seinfeld (2011) found no latent heating effect of increased CCN in a bulk scheme used to simulate idealised deep convection, whereas with a bin scheme increased latent heating aloft was demonstrated. However, Lebo et al. (2012) found that saturation adjustment methods used in bulk schemes could explain differences in the response of cold pool evolution and convective dynamics between bin and bulk schemes to aerosol loading, but could not explain large differences in the response of surface precipitation. Further, some simulations using bulk schemes have identified invigoration-like effects under aerosol loading. For example, Lebo and Morrison (2014) found evidence of convective invigoration under increased aerosol loading in a bulk scheme under weak shear conditions (and suppressed convection under strong shear), similar to the findings of Fan et al. (2009) who found the same response in a bin scheme. Seifert and Beheng (2006a) also found higher overshooting tops and larger sizes of cumulonimbus in a weak shear environment with increased aerosol loading. Thus although our results agree with the body of the literature which doesn not identify a convective updraught invigoration effect when bulk microphysics schemes are used, this is not necessarily attributable to the saturation adjustment method alone, and may also only hold for the particular convective environment (idealised supercell in strong shear) we consider.

3.3 WRF LES RICO~~: liquid-phase processes~~

The results presented in Sections 3.1 and 3.2 indicate that not only ~~do the simulated hydrometeor classes differ between microphysics schemes and between cases~~ is the way in which the schemes differ from each other not systematic between cases of convection, but that the ~~hydrometeor response to CDNC perturbations also differs between microphysics schemes and between cases~~difference between the response of the two schemes to CDNC across types of convection is also not systematic. The largest difference between the microphysics schemes in the real-data Congo basin simulations occurs in the liquid-phase hydrometeor development and response to CDNC. Making the assumption that the liquid phase is the first to respond to CDNC perturbations and the perturbation subsequently propagates to the ice phase, we consider a case of precipitating shallow cumulus convection to investigate the liquid-phase differences between the schemes. Note that the 'baseline' hydrometeor profiles in Figure 11 show data from the configurations using a prescribed CDNC value of 100 cm^{-3} (rather than the baseline value

of 250 cm^{-3} used in the Congo basin and idealised supercell deep convection cases in Figures 6 and 8), as this is more appropriate for a pristine marine environment. Even when we restrict our simulations to the liquid phase, differences in the simulated hydrometeor classes are evident. The dominant domain-mean difference between the two schemes in the RICO case is clearly in the rain profile, with RICO-T100 producing significantly more rain than RICO-M100. Very little rain is present in the RICO-M100 configuration (Fig. 11a,d), whilst the RICO-T100 configuration produces a peak domain-mean rain mass of about 10^{-6} kg kg^{-1} (Fig. 11b). The liquid cloud profile is similar in both schemes, with RICO-M100 forming more cloud mass than RICO-T100 between 805 and 775 hPa in both the domain-mean and hydrometeor class-mean sense (Fig. 11c,f).

The response of the hydrometeors to CDNC perturbations also differs between schemes in the warm-rain RICO case (Fig. 12). In the RICO-MORR configuration, domain-mean rain and cloud mass both decrease under polluted conditions, although the rain response is very weak (on the order of 10^{-8} kg kg^{-1}) and the dominant response is a reduction in liquid cloud mass (Fig. 12a). In contrast, a reduction in rain mass is the dominant hydrometeor response under polluted conditions in the RICO-THOM configuration, and the decrease is nearly two orders of magnitude greater than that in RICO-MORR (Fig. 12b). The liquid cloud response to polluted conditions in RICO-THOM is weaker than the rain response, but still stronger than the cloud response in RICO-MORR. Cloud mass decreases under polluted conditions between 935 and 825 hPa, but increases at higher levels (Fig. 12b). Note that once again, the response of the simulated hydrometeors to CDNC perturbations differs between cases: under polluted conditions, RICO-MORR exhibits a decrease in cloud and rain mass, while CONGO-MORR exhibits a decrease in rain mass with little reponse in the liquid cloud (Fig. 7a), and SUPER-MORR shows almost no liquid-phase response at all (Fig. 9a). Likewise, RICO-THOM exhibits a decrease in rain and increase in cloud mass under polluted conditions, while CONGO-THOM exhibits similar behaviour (Fig. 7b) but SUPER-THOM shows a decrease in rain mass with little response in the liquid cloud (Fig. 9b). When mean profiles of each hydrometeor class are considered, the two schemes actually show similar responses to CDNC (increased upper-level cloud mass and suppressed rain, Figs. 9c,d). This indicates that the main response to CDNC in this case is not through the individual microphysical processes but through the absolute amounts of cloud and rain that are generated.

To illustrate the difference in the strength of response of the schemes to CDNC, total accumulated surface rain is shown for each RICO configuration in Figure 13a, along with an extra configuration using a 'very pristine' CDNC value of 50 cm^{-3}, and a series of sensitivity tests that will be discussed later. The 50 cm^{-3} CDNC configuration has been added because even at a prescribed CDNC value of 100 cm^{-3} very little rain production occurs in the RICO-MORR configuration. Warm rain formation differs strongly between schemes: very low CDNC values are required for the RICO-MORR configuration to produce any rain, whereas RICO-THOM produces significantly more rain at all CDNC values (Fig 13a). Even under very pristine conditions, the RICO-M50 configuration produces an order of magnitude less rain than RICO-T50 (Fig 13a). The different schemes also respond differently to CDNC perturbations. Rain production in RICO-MORR (which produces much less rain than RICO-THOM) shuts down very quickly as CDNC is increased: rain amounts are on the order of 10^2 mm at a CDNC value of 50 cm^{-3}, 10^{1} mm at a CDNC value of 100 cm^{-3}, 10^{-1} mm at a CDNC value of 250 cm^{-3}, and rain production ceases

completely at a CDNC value of 2500 cm^{-3} (Fig 13a). In contrast, rain production persists for much larger CDNC values in RICO-THOM: rain amounts are on the order of 10^{3} mm at CDNC values of 50 cm^{-3}, 10^{2} mm at CDNC values of 100 cm^{-3}, 10^{1} mm at CDNC values of 250 cm^{-3}, and while rain amounts are very low at CDNC values of 2500 cm^{-3} (on the order of 10^{-5} mm), rain production has not shut down completely (Fig 13a).

3.4 Sensitivity tests

Gilmore and Straka (2008) showed that the rain rates predicted by different autoconversion formulae in bulk schemes can vary by orders of magnitude. Autoconversion is parameterised differently in the two microphysics schemes. The Thompson scheme follows an adaptation of Berry and Reinhardt (1974), while the Morrison scheme follows the method of Khairoutdinov and Kogan (2000). The autoconversion rates as a function of cloud water content for each of the model configurations are shown in Figure 14. Also shown is the cloud water content (up to the mean plus 2 standard deviations) of each configuration . It is immediately clear that the threshold cloud liquid content for autoconversion in the Morrison scheme (solid lines) is significantly lower than that in the Thompson scheme (dashed lines), i.e. rain production can occur at much lower cloud liquid water contents in Morrison. ~~However, small amounts of rain will be re-evapourated easily, and this may explain the rapid shutdown of rain production with increasing CDNC in the RICO-MORR case.~~ It is also clear from the mean, (mean+1 standard deviation) and (mean+2standard deviations) cloud water content limits that rain production through autoconversion ought to be possible in all model configurations. However, despite the higher cloud water content threshold for autoconversion in the Thompson scheme, autoconversion rates are much greater once the threshold is reached, and liquid cloud is converted to rain much faster in Thompson than in Morrison. From Figure 14, it appears that the threshold for autoconversion is unlikely to be reached very often in any of the T2500 cases. In the deep ~~convection configurations~~convective cases, rain can be generated through ice and mixed-phase processes, but in the RICO warm-rain case this cannot occur. This explains why, compared to more pristine conditions, cloud mass increases in RICO-T2500 while rain mass decreases (Figure 12b).

Because Figure 14 indicates that the autoconversion threshold may be at least in part responsible for this response in the RICO-THOM case, we replace the autoconversion parameterisation in the Morrison scheme with that from the Thompson scheme, and vice versa. We use the notation M100T to denote the Morrison microphysics scheme (at a CDNC value of 100 cm^{-3}) with Thompson autoconversion (that of Berry and Reinhardt, 1974), and T100M to denote the Thompson scheme with Morrison autoconversion (that of Khairoutdinov and Kogan, 2000). Differences in the domain-mean hydrometeor mixing ratio profiles for each of the autoconversion-swapped configurations in the RICO case are shown in Figure 15. It is immediately clear that, in the warm-rain configuration, simply swapping the autoconversion treatment makes the hydrometeor development of the microphysics schemes much more like each other. The difference between the RICO-M100 configuration with the Morrison and Thompson autoconversion parameterisations (Fig. 15a) is quantitatively and qualitatively very similar to the difference between the RICO-M100 and RICO-T100 configurations (Fig. 11c). Likewise, the difference between the RICO-T100 configuration with the Morrison and Thompson autoconversion parameterisations (Fig. 15b) and finally the difference between

the RICO-T100 configuration with the Morrison autoconversion parameterisation and the RICO-M100 configuration with the Thompson autoconversion parameterisation (Fig. 15c) are also very similar to the difference between the RICO-M100 and RICO-T100 configurations (Fig. 11c).

Similarly, swapping the autoconversion parameterisations between the microphysics schemes in the RICO cases makes the surface rain production of the microphysics schemes much more like each other. The accumulated surface rainfall in the RICO-M100T configuration looks much more similar to the surface rainfall in the RICO-T100 configuration than it does to the RICO-M100 configuration (Fig. 13a). Rain amounts are on the order of 10^2 mm in RICO-M100T and RICO-T100, whereas in RICO-M100 it is two orders of magnitude smaller (Fig. 13a). Likewise, the accumulated surface rainfall in the RICO-T100M configuration is of order 10^1 mm compared to 10^2 mm in the standard RICO-T100 case (Fig. 13a). To further test the importance of autoconversion in the liquid phase simulations, we first turn off autoconversion completely in the 100 cm^{-3} CDNC simulations, and then allow autoconversion to occur but prevent the accretion of cloud water by rain. By design, in the absence of ice processes ~~,~~ no precipitation occurs without autoconversion of cloud water to rain (Fig.13a, M100noAUTO and T100noAUTO). However, in the RICO 100 cm^{-3} CDNC liquid-phase configuration the Thompson scheme can produce surface rain from autoconversion alone (albeit two orders of magnitude less than when rain can also accrete cloud water, (Fig. 13a, T100noACCR and T100), showing that autoconversion acts almost like a "seed" in this scheme, after which accretion takes over the rain production process. In contrast, zero surface precipitation is produced in RICO M100noACCR (Fig. 13a), showing that in this (liquid-phase only) configuration the Morrison scheme requires both the autoconversion of cloud droplets to rain and the accretion of rain by cloud droplets in order to produce surface precipitation.

Despite the significant effect of autoconversion in the liquid-phase simulations, changing the autoconversion parameterisation in the idealised supercell case has very little effect on the hydrometeor development (results not shown). This is unsurprising, as ice and mixed-phase processes will dominate this shear-driven deep convective environment. However, the Congo basin configurations show large differences between microphysics schemes in the partioning of water into liquid and ice phases (CONGO-THOM produces much more liquid cloud; CONGO-MORR produces much more ice). In the CONGO-THOM configurations, the liquid-phase response to increased CDNC is also very similar to the RICO-THOM response (increased liquid cloud mass and decreased rain mass, Fig. 7b). When the Thompson autoconversion treatment is implemented in the Morrison scheme, rain production in the southern half of the domain ceases in CONGO-M250T, and the liquid phase is instead represented by low-level cloud with structure similar to the CONGO-T250 configuration (Figure 16a, compared to Figure 4e). To test if radiative effects associated with large amounts of anvil ice drive or contribute to the differences in low cloud, we also set the ice extinction coefficient to zero in both the longwave and shortwave radiation schemes in CONGO-M250. However, this has no effect on the low-cloud characteristics (Figure 16e compared to Figure 4b), and we therefore conclude that autoconversion of cloud water to rain is the factor dominating the absence of low-level cloud in the south of the domain in the CONGO-MORR simulations. In contrast, autoconversion is a less significant process in the CONGO-T250 configuration. Implementing the Morrison autoconversion treatment in the Thompson scheme has very little effect on the hydrometeor structure

in the CONGO-T250M configuration compared to the CONGO-M250 configuration (Figure 16b, compared to Figure 4b). As a final test, the autoconversion process is turned off in both of the microphysics schemes. This confirms that autoconversion dominates the lack of low cloud in CONGO-M250: the resulting liquid-phase hydrometeor structure (Figure 16c) is similar to both CONGO-T250 (Fig. 7b) and CONGO-M250T (Figure 16a). This also confirms that autoconversion is much less significant in the CONGO-THOM configurations: the bulk hydrometeor structure when autoconversion is turned off in CONGO-T250 (Figure 16d) is very similar to both CONGO-T250 (Fig. 7b) and CONGO-T250M (Figure 16b).

~~Our results~~ We have shown that the autoconversion process is responsible for the removal of the large cloud mass at low levels in the model configuration with the Morrison microphysics scheme. We also see that this low-level liquid phase cloud mass forms when we run the same simulation using the WRF bin microphysics implementation (the SBM part of the Hebrew University Cloud M although to a lesser extent than in the Thompson simulations, and the warm cloud produced by the WRF-SBM produces rain (Figs. S2 and S3 in the Supplement). We therefore suggest that it is not the Thompson scheme per se which is responsible for producing the low-level cloud mass, but rather the larger-scale meteorological conditions present in which these simulations are performed.

A further significant difference between the two schemes in the Congo simulations is the generation of large amounts of upper-level ice in CONGO-M250 which is not present in CONGO-T250 (Figs. 4b,e). In the Thompson scheme, the fraction of ice mass with a diameter greater than 125 μm is instantaneously transferred into the snow category (Thompson et al., 2008). The same threshold size for cloud ice autoconversion to snow is used in the Morrison scheme, but the process is parameterised differently (Morrison et al., 2005). Because the Morrison scheme appears to produce large amounts of anvil cloudiness for the Congo case, which is not seen in the observations (Figure 5), we perform further sensitivity tests in which we reduce the threshold size for cloud ice autoconversion in the Morrison scheme to 50% of its original value (Figure 16f), 10% of its original value (Figure 16g), and then finally replace the autoconversion of cloud ice to snow in the Morrison scheme with the parameterisation used in the Thompson scheme (Figure 16h). In all tests, the upper-level anvil ice is reduced significantly. Using the lowest value of the threshold size for cloud ice autoconversion reduces the anvil cloud, because almost all of the ice is immediately converted to snow (Figure 16g). However, using the Thompson ice autoconversion representation in the Morrison scheme significantly reduces the amount of cloud ice in the simulation, and all of the detrained anvil ice is removed (Figure 16h). This suggests that for the particular Congo simulation we have investigated, the conversion of cloud ice to snow is the main factor leading to the significant difference in anvil cloudiness between the two schemes, and is responsible for the difference in upper-level cloud between the CONGO-M250 simulation and the observations (Figure 5). Indeed, we note that in equivalent simulations performed with the WRF-SBM, the same persistent upper-level ice forms (Figure S2 in the Supplement). This shows that differences resulting from conversion of one ice category into another is a limitation of any scheme whether bin or bulk which uses fixed ice categories. Our results provide further evidence that the use of discrete ice-phase hydrometeor categories may be detrimental to the correct simulation of cloud, and suggests that new schemes which do not use such

partitioning may give better results (e.g. Morrison and Grabowski, 2008; Harrington et al., 2013; Morrison et al., 2015b).

Our results show little impact of aerosol on precipitation in the Congo basin (Fig. 2b, Fig. 7), which is also seen when considering total accumulated surface precipitation (Fig. 13b), although CONGO-T2500 exhibits weak preciptation suppression under polluted conditions). This may be due to the longer duration of these simulations, performed over a larger domain, allowing the interaction of many cloud systems rather than considering the lifetime of a single isolated cloud. However, we also see that although the representation of autoconversion has a significant effect on the vertical hydrometeor structure in the CONGO-M250 configurations (Fig. 4b, Fig. 16a and Fig. 16c), it has a much weaker effect on total surface precipitation (Fig. 13b, M250, T250, M250T, T250M, M250noAUTO and T250noAUTO). This is perhaps unsurprising, as the dominant contribution to the accumulated surface precipitation over the Congo domain will be from ice processes in the convective region and not from the liquid-phase cloud. Although the lack of impact of aerosol on precipitation in the Congo simulations may be due to the use of bulk schemes in this study for the reasons detailed in Khain et al. (2015), and perhaps a different response would be seen using a bin scheme (e.g. Khain and Lynn, 2009; Lebo and Seinfeld, 2011), other studies using bulk and bin-bulk schemes have identified aerosol impacts on precipitation of up to about 15% (e.g. van den Heever et al., 2006; Lee and Feingold, 2010; Lee, 2012; Morrison and Gr
Indeed, even studies using bin schemes have been shown to have little impact on total precipitation, although inducing a shift in rainfall rates (Fan et al., 2013). Therefore, we note again that the choice of microphysics scheme, rather than aerosol response in either scheme, is the dominant contribution to uncertainty in the total precipitation.

4 Discussion and Conclusions

~~In this study we used WRF coupled to~~ This study considered the cloud and precipitation development using two double-moment bulk microphysics schemes (Morrison et al., 2009; Thompson et al., 2008) to perform cloud system-resolving simulations of ~~convection in the Congo basin, an idealised supercell, and a case of shallow cumulus convection , and~~ 3 types of convection, two of which were idealised (one deep convection case with open boundaries and one shallow cumulus case with periodic boundaries), and one real-data case of deep convection in the Congo basin using meteorological initial and boundary conditions. We tested the sensitivity of the simulated hydrometeors and precipitation to the microphysics scheme and to CDNC perturbations. The simulations were performed to explore the uncertainty in cloud and precipitation development and response to aerosol perturbations in convection-permitting models that can arise from the microphysics representation. We find that the variability among the two schemes, including the response to aerosol, differs widely between these cases. Although previous studies have found large sensitivity to choice of microphysics schemes (e.g. Khain et al., 2015, 2016), we show this in a consistent setup by considering different cases with the same model and same CDNC values and constraining as many other possible sources of variability as is feasible. Our results show that for the bulk schemes used in these simulations, aerosol effects are dominated by the uncertainty in cloud and precipitation development which arises from the choice of microphysics

scheme. This result was true for multiple cloud types in multiple environmental conditions.

~~A key finding is that the simulated hydrometeor classes differ significantly between microphysics schemes. Another~~ A key finding is that the difference between the ~~hydrometeor classes simulated by each microphysics scheme varies between cases of convection.~~ two schemes, including their response to CDNC, in different environments and cloud types is not systematic. This could perhaps be related to the nonmonotonic response to aerosol in different environments found by Kalina et al. (2014) (although their study only considered simulations of idealised supercells with a single bulk scheme and four environmental soundings). This nonmonotonic response was attributed to compensating changes in the microphysical processes under polluted conditions.

The maximum relative difference in mass mixing ratio between each hydrometeor class in the M250 and T250 configurations for each case of convection is summarised in Table 3. Not only are the maximum differences in the domain-mean profiles of the hydrometeor classes simulated by each microphysics scheme on the order of at least tens of percent, but it is also clear that both the magnitude and sign of the difference varies between cases. In some cases, the magnitude of the difference is huge: most notably, in the Congo basin case the maximum difference in liquid cloud mass between the Morrison and Thompson schemes is on the order of 10^4 kg kg^{-1} more in Thompson (whereas in the RICO shallow cumulus case the maximum difference is on the order of 10^1 kg kg^{-1} less in Thompson). Likewise, in the RICO case the maximum difference in rain mass between the Morrison and Thompson schemes is on the order of 10^3 kg kg^{-1} more in Thompson (whereas in the Congo basin case the maximum difference is on the order of 10^1 kg kg^{-1} less in Thompson). Even for hydrometeors that have differences of the same order of magnitude, the sign of the difference can vary between cases. This result highlights the need for better observational constraints on mixed-phase and ice cloud microphysics and hydrometeors, and also perhaps the need for a shift in the development of microphysics parameterisations away from schemes which (somewhat arbitrarily) partition hydrometeors into separate categories. This is also supported by our sensitivity tests of autoconversion of cloud ice to snow in our Congo simulations.

Another key finding is that the cloud morphological difference and the difference in the hydrometeors between different schemes is significantly larger than that due to CDNC perturbations. Although we have restricted our study to the comparison of double-moment bulk microphysics schemes, this result is consistent with Khain and Lynn (2009), who found that the difference in convection between a bulk and a bin scheme was much greater than the difference within each scheme to varying aerosol concentrations. Some studies have found a significantly weaker response to aerosol when using bulk schemes compared to bin schemes, e.g. Khain and Lynn (2009); Lebo and Seinfeld (2011). In idealised simulations of continental deep convection, Lebo and Seinfeld (2011) found that increases in CCN concentrations led to increased ice mass and total condensed water mass aloft in both bin and bulk schemes, but increased surface domain-averaged cumulative surface precipitation in the bulk scheme compared to a decrease in the bin scheme. This was shown to be because the relative increase in condensate mass aloft under polluted conditions was found to be much larger in the simulations performed with bulk microphysics, a result of increased numbers of smaller cloud particles with slower sedimentation speeds, thus resulting in reduced surface precipitation.

However, in our idealised supercell simulations we find a similar magnitude of response to aerosol when using a bin scheme as the response in the two bulk schemes which are the focus of this study.

That cloud and precipitation development and their aerosol response differs across different cloud types in different large-scale environments is expected. Many studies have shown that aerosol effects on precipitation depend on the large-scale environment and cloud type (e.g. Khain et al., 2004; Fan et al., 2007b; Lynn et al., 2005a, b; Lynn and Khain, 2007; Seifert and Beheng, 2006a; Tao et a for reasons related to differences in different cloud types between the timescale of increased sedimentation through aerosol loading and subsequent sublimation and evaporation timescales. Further, several studies of deep convection have found that the effects of aerosol on deep convection are much weaker than that of relative humidity (e.g. van den Heever et al., 2006; Fan et al., 2007a; Kh Fan et al. (2007b) found that in idealised simulations of continental and maritime clouds using bin microphysics the magnitude and even the sign of aerosol effects on precipitation depended on relative humidity. Fan et al. (2007a) found that aerosol response in idealised simulations of clouds using bin microphysics and soundings from Houston, Texas strongly depended on relative humidity, having negligible effect on cloud properties and precipitation in dry air but more significant effects in humid air. Conversely, in idealised low-precipitation supercell simulations with bulk microphysics and dry low-level humidity performed as part of the study by Kalina et al. 2014, cold pool area decreased by 84% and domain-averaged precipitation reduced by 50% under polluted conditions whereas it was insensitive to polluted conditions when a moist sounding was used. Thus, assuming that the response in our simulations would likely be more similar to the results found for bulk microphysics by Kalina et al. (2014) the magnitude of our results in the supercell case (which uses a moist sounding) may be smaller than it would be in drier environmental conditions.

In 10 day simulations of deep convection in the Congo basin in August 2007, we find that both the Morrison and Thompson schemes have a significant positive bias in cloud and surface precipitation compared to GERB and TRMM. This may be in part attributable to the positive moist bias in the Congo basin in the ERA-Interim reanalysis (used as boundary data for the Congo simulation) when compared to other reanalyses (Washington et al., 2013). Despite the positive cloud fraction bias in both schemes, we find that the Thompson scheme compares better than the Morrison scheme against observed cloud fractions, largely due to the overproduction of upper-level ice in the Morrison scheme. This is in agreement with Cintineo et al. (2014), who found that (despite the two schemes having different biases at different levels) the Thompson scheme outperformed the Morrison scheme overall against satellite observations of cloud in North America due to its more accurate upper-level cloud distribution, whereas the Morrison scheme had too much upper-level cloud through overproduction of ice. This ~~could be attributable purely to the upper limits on ice number concentrations used in each scheme rather than to a more accurate description of ice-phase processes. The version of the Morrison scheme used in this study limits ice number concentrations to 0.3 cm^{-3}, whereas the Thompson scheme has an upper limit on ice number concentration a full order of magnitude smaller~~bias is attributable to differences in the way in which the two schemes convert cloud ice to snow. However, we also find that despite a positive surface precipitation bias in both schemes, the Morrison scheme compares better to observations in this region over this period. ~~This therefore~~ Morrison and Grabowski (2007) found that differences in accumulated precipitation produced by warm

stratocumulus and warm cumulus clouds using different microphysics schemes were only on the order of 10 to 20%, suggesting that accumulated rain is largely controlled by large-scale atmospheric properties. However, differences in accumulated rain in our Congo simulations can be attributed to differences in the microphysics schemes, because all simulations used the same input and boundary data and therefore are under the influence of the same large-scale atmospheric conditions. That one scheme best represents cold cloud compared to observations but the other scheme better reproduces accumulated precipitation makes it difficult to conclude that one scheme outperforms another overall, and suggests that when setting up a model configuration for research purposes, ~~the choice of which scheme to use may best be guided as to~~ one consideration to distinguish between the use of these two particular schemes may be whether surface precipitation or radiative effects are more important to the research question.

~~Another key finding is that the cloud morphological difference and the difference in the hydrometeors between different schemes is significantly larger than that due to CDNC perturbations. Although we have restricted our study to the comparison of double-moment bulk microphysics schemes, this result is consistent with Khain and Lynn (2009), who found that the difference in convection between a bulk and a bin scheme was much greater than the difference within each scheme to varying aerosol concentrations.~~ We note here that the RRTM LW and Goddard SW radiation schemes used in these simulations are only coupled to the microphysics through the hydrometeor masses and not the numbers. This coupling therefore cannot account for changes in hydrometeor sizes, and thus some aerosol effects will be missing from these simulations. Additionally, the microphysics-radiation coupling is only through cloud water and ice, and none of the other frozen species. This missing aerosol effect may have an especially important impact in our Congo simulations, where the Morrison scheme develops and retains significant amounts of upper-level ice, whereas the Thompson scheme converts nearly all the ice to snow, which the radiation scheme will not see. This could have significant radiative flux and feedback impacts (Thompson et al., 2016), which in itself originates from the use of somewhat arbitrarily defined ice categories (e.g. if the size parameter at which cloud ice is converted to snow is changed, a bulk mass of cloud ice is removed from the radiatively-coupled ice category and moved into the non-radiatively coupled snow category).

We present the new result that ~~the response of the hydrometeors to CDNC perturbations~~ variabilty in aerosol response due to choice of microphysics scheme differs not just between schemes, but ~~is also case-dependent for each scheme~~that the inter-scheme variability differs between cases of convection. The maximum relative difference in the domain-mean hydrometeor profiles between polluted and pristine CDNC values for each of the model configurations is summarised in Table 4. It is clear that both the magnitude and the sign of the reponse of each hydrometeor class to CDNC differs strongly not just between microphysics schemes, but also between cases. (Note that Table 4 shows relative amounts, and that the absolute difference in response to CDNC between each of the schemes and cases can also vary significantly).

Whilst it is not surprising that the different cases of convection differ in their hydrometeor development and in their response to polluted conditions, it is worth noting the magnitude and variation of the difference in response. A body of literature uses idealised model configurations to investigate storm-system response to aerosol loading (e.g. Seifert and Beheng, 2006b; Khain and

Lynn, 2009; Lebo and Seinfeld, 2011; Morrison, 2012) and to compare microphysics schemes (e.g. Lebo and Seinfeld, 2011). Our results highlight that the storm-system response in such a model configuration may not be representative of the response over larger spatiotemporal scales, supporting similar findings of larger-scale feedbacks and lifecycle-dependent responses in idealised (Morrison and Grabowski, 2011; Lee, 2012) and real-data (van den Heever et al., 2006) studies of aerosol–convection interations.

We ~~emphasize that the nature of our study is highly idealised: neither microphysics scheme treats cloud processing of aerosol, and thus we expect that the magnitude of the cloud repsonse to polluted conditions found in our study provides an upper limit on that which would result if processes such as wet deposition or other buffering processes (e.g. Stevens and Feingold, 2009; Seifert and Behen accounted for. However, we note firstly that the highly different response of each of the schemes in each of the cases has significant implications for studies of aerosol effects on convection. Many aerosol–convection interaction studies compare the response to aerosol (or some proxy variable for aerosol) of a single model configuration of deep convection coupled to a single microphysics parameterisation (e.g. Lim et al., 2011). Considering the growing body of literature of aerosol–convection process interactions, our study shows that additional constraints are needed to allow us to reliably compare any studies that do not use exactly the same model and model configuration. Secondly, we note that although our results represent an upper limit on the uncertainties that exist between different configurations of the same model, the fact that the uncertainty exists highlights fundamental deficiencies in our understanding of cloud microphysical processes. Adding complexity to our models to represent processes that may dampen this uncertainty (e.g. wet deposition) without first addressing the uncertainties themselves would amount to making the model behave 'more correctly' simply by masking errors in the model physics.~~

~~We note that the~~ note that the vertical resolution used in this study is relatively coarse, and that a horizontal grid length of 4 km is at the limit of what may be considered as 'convection-permitting' (Bryan et al., 2003). However, we use this grid spacing for consistency with a previous study, where 10 km and 4 km grid lengths were shown to be sufficient to reproduce storm characteristics and aerosol–convection interactions in the Congo basin (Gryspeerdt et al., 2015). Previous studies have indicated sensitivity of convection to horizontal grid spacing (e.g. Bryan and Morrison, 2012; Potvin and Flora, 2015) and also that the sensitivity to grid length can vary with microphysics scheme (Morrison et al., 2015b), although idealised ensemble studies of response to aerosol have shown that differences between polluted and pristine conditions were similar in simulations using horizontal grid lengths of 4 km, 2 km, and 0.5 km, respectively and were also relatively robust to domain size (Morrison and Grabowski, 2011). ~~A full systematic study of the sensitivity of convective development and of aerosol indirect effects to horizontal and vertical resolution, to domain size, and to microphysics parameterisation, is beyond the scope of the current study but remains a focus of ongoing work~~

An important factor in our setup is that we use the same values of prescribed CDNC in all of our cases. Whilst the literature also shows widely varying response to aerosol, especially between bin and bulk schemes (where even the sign of the response may differ), Kalina et al. (2014) showed in idealised supercell simulations using 15 CCN concentrations and 4 environmental soundings that changes in cold pool characteristics with CCN were nonmonotonic and dependent on the environmental

conditions. Therefore our use of the same CDNC values in multiple types of convection helps to minimise uncertainty due to nonmonotonic behvaiour. However, considering the results of Kalina et al. (2014), we note that a caveat of the present study (and indeed of the majority of existing studies) is that the absolute values of the cloud system and precipitation response to aerosol identified here may only hold for the CDNC values used in our study.

We find that the autoconversion representation alone is sufficient to explain most of the differences between microphysics schemes in the shallow cumulus case both in terms of their representation of cloud and precipitation ~~(consistent with Li et al., 2015)~~ (consis also in terms of their response to CDNC. The dominant hydrometeor difference between the microphysics schemes in the RICO simulations occurs in the rain - a different result from both the Congo basin configuration (where the dominant difference occurs in the liquid cloud) and the idealised supercell configuration (where the dominant difference occurs in the graupel). We also find that autoconversion of cloud droplets to rain is the mechanism that prevents the formation (or persistence) of liquid-phase cloud in the south of the domain in the Congo basin simulations using the Morrison scheme. This is in agreement with the study of Kalina et al. (2014), who found in idealised supercell simulations using the Morrison bulk microphysics scheme with a variable shape parameter for the raindrop size distribution that autoconversion rates decreased under CCN loading. The importance of autoconversion representation was shown by Gilmore and Straka (2008), who showed that the rates predicted by the autoconversion formulae used in bulk schemes differ by orders of magnitude. Modelling studies and observations from RICO have found that warm rain formation can be explained by the observed aerosol distribution (Blyth et al., 2013). In the context of our findings, this strongly suggests that an accurate description of the autoconversion process in warm-rain regimes is fundamental not only to a realistic representation of cloud and precipitation, but also to its response to varying aerosol concentrations.

Our results (which are shown to hold across multiple cloud types and types of simulation) have important implications not just for cloud-resolving simulations but also for the global modelling community. Most significant, perhaps, is then the radiative impact which could arise when such major differences occur in the ice phase. Our Congo simulations illustrate just how large this uncertainty may be, and our tests using a bin scheme show that this is not purely an artefact of the bulk microphysics schemes used. Further, that uncertainties due to choice of microphysics scheme dominate any aerosol response within a given scheme has implications for global modelling studies of aerosol indirect effects (e.g. Zhang et al., 2016; Ghan et al., 2016). Once again, this highlights the continuing need of our community for tight observational contraints on cloud and precipitation processes and their repsonse to aerosol, and for ongoing parameterisation development to allow these processes to be accurately represented in large-domain (or global), long-term simulations.

~~The analysis provided here adds to the body of literature that explores the response of convection-permitting simulations to aerosol perturbations. Our study helps to bridge the gap in the literature between studies of a single precipitation event using multiple microphysics schemes and studies investigating the response of a single scheme to CDNC or CCN perturbations, and is the first such study to consider multiple cases of convection. This work highlights the large uncertainty in cloud morphology,~~

~~hydrometeor development and response to CDNC that can result not just from different microphysics representations but also in different cases of convection, and indicates the ongoing need for stronger observational constraints on hydrometeors and microphysical processes.~~

Acknowledgements. This work used the ARCHER UK National Supercomputing Service (http://www.archer.ac.uk). The research leading to these results has received funding from the European Research Council under the European Union's Seventh Framework Programme (FP7/2007–2013)/ERC grant agreement no. FP7- 280025 (ACCLAIM) and grant agreement no. FP7- 306284 (QUARERE). The Congo precipitation data used in this study were acquired as part of the Tropical Rainfall Measuring Mission (TRMM). The algorithms were developed by the TRMM Science Team. The data were processed by the TRMM Science Data and Information System (TSDIS) and the TRMM office; they are archived and distributed by the Goddard Distributed Active Archive Center. TRMM is an international project jointly sponsored by the Japan National Space Development Agency (NASDA) and the US National Aeronautics and Space Administration (NASA) Office of Earth Sciences. The Congo radiance data used in this study were acquired as part of the Geostationary Earth Radiation Budget Project. The CloudSat data was obtained from the CloudSat Data Processing Center. ERA-Interim data provided courtesy ECMWF. Thanks go to Zak Kipling and Laurent Labbouz (University of Oxford, UK) for helpful comments on this manuscript.

References

Albrecht, B.: Aerosols, Cloud Microphysics, and Fractional Cloudiness, Science, 245, 1227–1230, 1989.

Altaratz, O., Koren, I., Remer, L., and Hirsch, E.: Review: Cloud invigoration by aerosols—Coupling between microphysics and dynamics, Atmospheric Research, 140–141, 38 – 60, doi:http://dx.doi.org/10.1016/j.atmosres.2014.01.009, http://www.sciencedirect.com/science/article/pii/S0169809514000106, 2014.

Beljaars, A.: The parameterization of surface fluxes in large-scale models under free convection, Quarterly Journal of the Royal Meteorological Society, 121, 225–270, 1994.

Berry, E. and Reinhardt, R.: An Analysis of Cloud Drop Growth by Collection: Part I. Double Distributions, J. Atmos. Sci., 31, 1814—-1824, 1974.

Blyth, A., Lowenstein, J., Huang, Y., Cui, Z., Davies, S., and Carslaw, K.: The production of warm rain in shallowmaritime cumulus clouds, Quarterly Journal of the Royal Meteorological Society, 139, 20–31, 2013.

Bryan, G. and Morrison, H.: Sensitivity of a Simulated Squall Line to Horizontal Resolution and Parameterization of Microphysics, Mon. Wea. Rev., 140, 202—-225, doi:http://dx.doi.org/10.1175/MWR-D-11-00046.1, 2012.

Bryan, G., Wyngaard, J., and Fritsch, J.: Resolution Requirements for the Simulation of Deep Moist Convection, Mon. Wea. Rev., 131, 2394—2416, doi:http://dx.doi.org/10.1175/1520-0493(2003)131<2394:RRFTSO>2.0.CO;2, 2003.

Chand, D., Wood, R., Ghan, S. J., Wang, M., Ovchinnikov, M., Rasch, P. J., Miller, S., Schichtel, B., and Moore, T.: Aerosol optical depth increase in partly cloudy conditions, Journal of Geophysical Research: Atmospheres, 117, 2012.

Chou, M.-D. and Suarez, M.: An efficient thermal infrared radiation parameterization for use in general circulation models, NASA Technical Memo, 1994.

Cintineo, R., Otkin, J. A., Xue, M., and Kong, F.: Evaluating the Performance of Planetary Boundary Layer and Cloud Microphysical Parameterization Schemes in Convection-Permitting Ensemble Forecasts Using Synthetic GOES-13 Satellite Observations, Monthly Weather Review, 142, 163–182, 2014.

Dee, D. P., Uppala, S. M., Simmons, A. J., Berrisford, P., Poli, P., Kobayashi, S., Andrae, U., Balmaseda, M. A., Balsamo, G., Bauer, P., Bechtold, P., Beljaars, A. C. M., van de Berg, L., Bidlot, J., Bormann, N., Delsol, C., Dragani, R., Fuentes, M., Geer, A. J., Haimberger, L., Healy, S. B., Hersbach, H., Hólm, E. V., Isaksen, L., Kållberg, P., Köhler, M., Matricardi, M., McNally, A. P., Monge-Sanz, B. M., Morcrette, J.-J., Park, B.-K., Peubey, C., de Rosnay, P., Tavolato, C., Thépaut, J.-N., and Vitart, F.: The ERA-Interim reanalysis: configuration and performance of the data assimilation system, Quarterly Journal of the Royal Meteorological Society, 137, 553–597, 2011.

Dyer, A. and Hicks, B.: Flux-gradient relationships in the constant flux layer, Quarterly Journal of the Royal Meteorological Society, 96, 715–721, 1970.

Ek, M. and Mahrt, L.: SU 1-D PBL Model User's Guide. Version1.04, Department of Atmospheric Sciences, Oregon State University, 1991.

Fan, J., Zhang, R., Li, G., and Tao, W.-K.: Effects of aerosols and relative humidity on cumulus clouds, Journal of Geophysical Research: Atmospheres, 112, doi:10.1029/2006JD008136, http://dx.doi.org/10.1029/2006JD008136, 2007a.

Fan, J., Zhang, R., Li, G., and Tao, W.-K.: Effects of aerosols and relative humidity on cumulus clouds, Journal of Geophysical Research: Atmospheres, 112, doi:10.1029/2006JD008136, http://dx.doi.org/10.1029/2006JD008136, 2007b.

Fan, J., Yuan, T., Comstock, J. M., Ghan, S., Khain, A., Leung, L. R., Li, Z., Martins, V. J., and Ovchinnikov, M.: Dominant role by vertical wind shear in regulating aerosol effects on deep convective clouds, Journal of Geophysical Research: Atmospheres, 114, n/a–n/a, 2009.

Fan, J., Leung, L. R., Li, Z., Morrison, H., Chen, H., Zhou, Y., Qian, Y., and Wang, Y.: Aerosol impacts on clouds and precipitation in eastern China: Results from bin and bulk microphysics, Journal of Geophysical Research: Atmospheres, 117, 2012a.

Fan, J., Rosenfeld, D., Ding, Y., Leung, L. R., and Li, Z.: Potential aerosol indirect effects on atmospheric circulation and radiative forcing through deep convection, Geophysical Research Letters, 39, n/a–n/a, doi:10.1029/2012GL051851, http://dx.doi.org/10.1029/2012GL051851, 2012b.

Fan, J., Leung, L. R., Rosenfeld, D., Chen, Q., Li, Z., Zhang, J., and Yan, H.: Microphysical effects determine macrophysical response for aerosol impacts on deep convective clouds, Proceedings of the National Academy of Sciences, 110, E4581–E4590, 2013.

Feingold, G., Stevens, B., Cotton, W., and Walko, R.: An explicit cloud microphysics/LES model designed to simulate the Twomey effect, Atmospheric Research, 33, 207 – 233, 1994.

Gallus Jr., W. A. and Pfeifer, M.: Intercomparison of simulations using 5 WRF microphysical schemes with dual-Polarization data for a German squall line, Advances in Geosciences, 16, 109–116, doi:10.5194/adgeo-16-109-2008, http://www.adv-geosci.net/16/109/2008/, 2008.

Ghan, S., Wang, M., Zhang, S., Ferrachat, S., Gettelman, A., Griesfeller, J., Kipling, Z., Lohmann, U., Morrison, H., Neubauer, D., Partridge, D. G., Stier, P., Takemura, T., Wang, H., and Zhang, K.: Challenges in constraining anthropogenic aerosol effects on cloud radiative forcing using present-day spatiotemporal variability, Proceedings of the National Academy of Sciences, 113, 5804–5811, doi:10.1073/pnas.1514036113, http://www.pnas.org/content/113/21/5804.abstract, 2016.

Gilmore, M. S. and Straka, J. M.: The Berry and Reinhardt Autoconversion Parameterization: A Digest, Journal of Applied Meteorology and Climatology, 47, 375–396, doi:10.1175/2007JAMC1573.1, http://dx.doi.org/10.1175/2007JAMC1573.1, 2008.

Gryspeerdt, E., Stier, P., and Partridge, D. G.: Links between satellite-retrieved aerosol and precipitation, Atmospheric Chemistry and Physics, 14, 9677–9694, 2014.

Gryspeerdt, E., Stier, P., White, B. A., and Kipling, Z.: Wet scavenging limits the detection of aerosol effects on precipitation, Atmospheric Chemistry and Physics, 15, 7557–7570, doi:10.5194/acp-15-7557-2015, http://www.atmos-chem-phys.net/15/7557/2015/, 2015.

Harries, J., Russell, J., Hanafin, J., Brindley, H., Futyan, J., Rufus, J., Kellock, S., Matthews, G., Wrigley, R., Last, A., Mueller, J., Mossavati, R., Ashmall, J., Sawyer, E., Parker, D., Caldwell, M., Allan, P., Smith, A., Bates, M., Coan, B., Stewart, B., Lepine, D., Cornwall, L., Corney, D., Ricketts, M., Drummond, D., Smart, D., Cutler, R., Dewitte, S., Clerbaux, N., Gonzalez, L., Ipe, A., Bertrand, C., Joukoff, A., Crommelynck, D., Nelms, N., Llewellyn-Jones, D., Butcher, G., Smith, G., Szewczyk, Z., Mlynczak, P., Slingo, A., Allan, R., and Ringer, M.: The geostationary Earth Radiation Budget Project, BULLETIN OF THE AMERICAN METEOROLOGICAL SOCIETY, 86, 945–+, doi:10.1175/BAMS-86-7-945, 2005.

Harrington, J. Y., Sulia, K., and Morrison, H.: A Method for Adaptive Habit Prediction in Bulk Microphysical Models. Part I: Theoretical Development, Journal of the Atmospheric Sciences, 70, 349–364, 2013.

Haynes, J. M., Luo, Z., Stephens, G. L., Marchand, R. T., and Bodas-Salcedo, A.: A Multipurpose Radar Simulation Package: QuickBeam, Bulletin of the American Meteorological Society, 88, 1723–1727, doi:10.1175/BAMS-88-11-1723, 2007.

Hong, S.-Y., Noh, Y., and Dudhia, J.: A new vertical diffusion package with explicit treatment of entrainment processes, Mon. Wea. Rev., 134, 2318–2341, 2006.

Hong, S.-Y., Lim, K.-S. S., Kim, J.-H., Lim, J.-O. J., and Dudhia, J.: Sensitivity Study of Cloud-Resolving Convective Simulations with WRF Using Two Bulk Microphysical Parameterizations: Ice-Phase Microphysics versus Sedimentation Effects, Journal of Applied Meteorology and Climatology, 48, 61–76, 2009.

Huffman, G. J., Adler, R. F., Bolvin, D. T., Gu, G., Nelkin, E. J., Bowman, K. P., Hong, Y., Stocker, E. F., David, and Wolff, B.: The TRMM Multi-satellite Precipitation Analysis: Quasi-Global, Multi-Year, Combined-Sensor Precipitation Estimates at Fine Scale, J. Hydrometeor, pp. 38–55, 2007.

Igel, A., Igel, M., and van den Heever, S.: Make It a Double? Sobering Results from Simulations Using Single-Moment Microphysics Schemes, J. Atmos. Sci., 72, 910–925, doi:10.1175/JAS-D-14-0107.1, 2015.

Jankov, I., Grasso, L., Sengupta, M., Neiman, P., Zupanski, D., Zupanski, M., Lindsey, D., Hillger, D., Birkenheuer, D., Brummer, R., and Yuan, H.: An evaluation of five arw-wrf microphysics schemes using synthetic goes imagery for an atmospheric river event affecting the california coast, J. Hydrometeor, 12, 618—-633, doi:http://dx.doi.org/10.1175/2010JHM1282.1, 2011.

Jiang, H., Cotton, W., Pinto, J., Curry, J., and Weissbluth, M.: Cloud Resolving Simulations of Mixed-Phase Arctic Stratus Observed during BASE: Sensitivity to Concentration of Ice Crystals and Large-Scale Heat and Moisture Advection, J. Atmos. Sci., 57, 2105—-2117, doi:http://dx.doi.org/10.1175/1520-0469(2000)057<2105:CRSOMP>2.0.CO;2, 2000.

Kalina, E. A., Friedrich, K., Morrison, H., and Bryan, G. H.: Aerosol Effects on Idealized Supercell Thunderstorms in Different Environments, Journal of the Atmospheric Sciences, 71, 4558–4580, doi:10.1175/JAS-D-14-0037.1, http://dx.doi.org/10.1175/JAS-D-14-0037.1, 2014.

Kessler, E. I.: On the distribution and continuity of water substance in atmospheric circulations, Meteorological Monographs, 1969.

Khain, A. and Lynn, B.: Simulation of a supercell storm in clean and dirty atmosphere using weather research and forecast model with spectral bin microphysics, Journal of Geophysical Research: Atmospheres, 114, 2009.

Khain, A., Pokrovsky, A., Pinsky, M., Seifert, A., and Phillips, V.: Simulation of Effects of Atmospheric Aerosols on Deep Turbulent Convective Clouds Using a Spectral Microphysics Mixed-Phase Cumulus Cloud Model. Part I: Model Description and Possible Applications, J. Atmos. Sci., 61, 2963—-2982, 2004.

Khain, A., Rosenfeld, D., Pokrovsky, A., Blahak, U., and Ryzhkov, A.: The role of {CCN} in precipitation and hail in a mid-latitude storm as seen in simulations using a spectral (bin) microphysics model in a 2D dynamic frame, Atmospheric Research, 99, 129 – 146, doi:http://dx.doi.org/10.1016/j.atmosres.2010.09.015, http://www.sciencedirect.com/science/article/pii/S016980951000253X, 2011.

Khain, A., Lynn, B., and Shpund, J.: High resolution {WRF} simulations of Hurricane Irene: Sensitivity to aerosols and choice of microphysical schemes, Atmospheric Research, 167, 129 – 145, doi:http://dx.doi.org/10.1016/j.atmosres.2015.07.014, http://www.sciencedirect.com/science/article/pii/S0169809515002264, 2016.

Khain, A. P., Beheng, K. D., Heymsfield, A., Korolev, A., Krichak, S. O., Levin, Z., Pinsky, M., Phillips, V., Prabhakaran, T., Teller, A., van den Heever, S. C., and Yano, J.-I.: Representation of microphysical processes in cloud-resolving models: Spectral (bin) microphysics versus bulk parameterization, Reviews of Geophysics, 53, 247–322, doi:10.1002/2014RG000468, 2015.

Khairoutdinov, M. and Kogan, Y.: A New Cloud Physics Parameterization in a Large-Eddy Simulation Model of Marine Stratocumulus, Mon. Wea. Rev., 128, 229—-243, 2000.

Koren, I., Kaufman, Y. J., Rosenfeld, D., Remer, L. A., and Rudich, Y.: Aerosol invigoration and restructuring of Atlantic convective clouds, Geophysical Research Letters, 32, doi:10.1029/2005GL023187, 2005.

Kumjian, M. R. and Ryzhkov, A. V.: The Impact of Size Sorting on the Polarimetric Radar Variables, Journal of the Atmospheric Sciences, 69, 2042–2060, doi:10.1175/JAS-D-11-0125.1, http://dx.doi.org/10.1175/JAS-D-11-0125.1, 2012.

Lebo, Z. J. and Morrison, H.: Dynamical Effects of Aerosol Perturbations on Simulated Idealized Squall Lines, Monthly Weather Review, 142, 991–1009, 2014.

Lebo, Z. J. and Seinfeld, J. H.: Theoretical basis for convective invigoration due to increased aerosol concentration, Atmospheric Chemistry and Physics, 11, 5407–5429, 2011.

Lebo, Z. J., Morrison, H., and Seinfeld, J. H.: Are simulated aerosol-induced effects on deep convective clouds strongly dependent on saturation adjustment?, Atmospheric Chemistry and Physics, 12, 9941–9964, doi:10.5194/acp-12-9941-2012, 2012.

Lee, S.-S.: Effect of aerosol on circulations and precipitation in deep convective clouds, J. Atmos. Sci., 69, 1957—-1974, 2012.

Lee, S.-S. and Feingold, G.: Precipitating cloud-system response to aerosol perturbations, Geophysical Research Letters, 37, 2010.

Lee, S.-S. and Feingold, G.: Aerosol effects on the cloud-field properties of tropical convective clouds, Atmospheric Chemistry and Physics, 13, 6713–6726, doi:10.5194/acp-13-6713-2013, http://www.atmos-chem-phys.net/13/6713/2013/, 2013.

Li, X., Tao, W.-K., Khain, A. P., Simpson, J., and Johnson, D. E.: Sensitivity of a Cloud-Resolving Model to Bulk and Explicit Bin Microphysical Schemes. Part I: Comparisons, Journal of the Atmospheric Sciences, 66, 3–21, doi:10.1175/2008JAS2646.1, http://dx.doi.org/10.1175/2008JAS2646.1, 2009a.

Li, X., Tao, W.-K., Khain, A. P., Simpson, J., and Johnson, D. E.: Sensitivity of a Cloud-Resolving Model to Bulk and Explicit Bin Microphysical Schemes. Part II: Cloud Microphysics and Storm Dynamics Interactions, Journal of the Atmospheric Sciences, 66, 22–40, doi:10.1175/2008JAS2647.1, http://dx.doi.org/10.1175/2008JAS2647.1, 2009b.

Li, Z., Zuidema, P., Zhu, P., and Morrison, H.: The Sensitivity of Simulated Shallow Cumulus Convection and Cold Pools to Microphysics, J. Atmos. Sci., 72, 3340–3355, 2015.

Lim, K.-S. S., Hong, S.-Y., Yum, S. S., Dudhia, J., and Klemp, J. B.: Aerosol effects on the development of a supercell storm in a double-moment bulk-cloud microphysics scheme, Journal of Geophysical Research: Atmospheres, 116, doi:10.1029/2010JD014128, d02204, 2011.

Lin, Y.-L., Farley, R., and Orville, H.: Bulk Parameterization of the Snow Field in a Cloud Model, J. Climate Appl. Meteor., 22, 1065—-1092, doi:http://dx.doi.org/10.1175/1520-0450(1983)022<1065:BPOTSF>2.0.CO;2, 1983.

Loftus, A. and Cotton, W.: Examination of {CCN} impacts on hail in a simulated supercell storm with triple-moment hail bulk microphysics, Atmospheric Research, 147–148, 183 – 204, doi:http://dx.doi.org/10.1016/j.atmosres.2014.04.017, 2014.

Lynn, B. and Khain, A.: Utilization of spectral bin microphysics and bulk parameterization schemes to simulate the cloud structure and precipitation in a mesoscale rain event, Journal of Geophysical Research: Atmospheres, 112, doi:10.1029/2007JD008475, http://dx.doi.org/10.1029/2007JD008475, 2007.

Lynn, B. H., Khain, A. P., Dudhia, J., Rosenfeld, D., Pokrovsky, A., and Seifert, A.: Spectral (Bin) Microphysics Coupled with a Mesoscale Model (MM5). Part I: Model Description and First Results, Monthly Weather Review, 133, 44–58, doi:10.1175/MWR-2840.1, http://dx.doi.org/10.1175/MWR-2840.1, 2005a.

Lynn, B. H., Khain, A. P., Dudhia, J., Rosenfeld, D., Pokrovsky, A., and Seifert, A.: Spectral (Bin) Microphysics Coupled with a Mesoscale Model (MM5). Part II: Simulation of a CaPE Rain Event with a Squall Line, Monthly Weather Review, 133, 59–71, doi:10.1175/MWR-2841.1, http://dx.doi.org/10.1175/MWR-2841.1, 2005b.

Marchand, R., Mace, G. G., Ackerman, T., and Stephens, G.: Hydrometeor Detection Using Cloudsat—An Earth-Orbiting 94-GHz Cloud Radar, Journal of Atmospheric and Oceanic Technology, 25, 519–533, doi:10.1175/2007JTECHA1006.1, 2008.

Mauger, G. S. and Norris, J. R.: Meteorological bias in satellite estimates of aerosol-cloud relationships, Geophysical Research Letters, 34, 2007.

McFarquhar, G. M., Zhang, H., Heymsfield, G., Halverson, J. B., Hood, R., Dudhia, J., and Jr., F. M.: Factors Affecting the Evolution of Hurricane Erin (2001) and the Distributions of Hydrometeors: Role of Microphysical Processes, Journal of the Atmospheric Sciences, 63, 127–150, 2006.

Meyers, M. P., Walko, R. L., Harrington, J. Y., and Cotton, W. R.: New {RAMS} cloud microphysics parameterization. Part {II}: The two-moment scheme, Atmospheric Research, 45, 3 – 39, doi:http://dx.doi.org/10.1016/S0169-8095(97)00018-5, 1997.

Milbrandt, J. A. and Yau, M. K.: A Multimoment Bulk Microphysics Parameterization. Part III: Control Simulation of a Hailstorm, Journal of the Atmospheric Sciences, 63, 3114–3136, doi:10.1175/JAS3816.1, 2006.

Mlawer, E., Taubman, S., Brown, P., Iacono, M., and Clough, S.: Radiative transfer for inhomogeneous atmospheres: RRTM, a validated correlated k-model for the longwave, Journal of Geophysical Research, 102, 1997.

Morrison, H.: On the robustness of aerosol effects on an idealized supercell storm simulated with a cloud system-resolving model, Atmos. Chem. Phys., 12, 7689–7705, doi:10.5194/acp-12-7689-2012, 2012.

Morrison, H. and Grabowski, W. W.: Comparison of Bulk and Bin Warm-Rain Microphysics Models Using a Kinematic Framework, Journal of the Atmospheric Sciences, 64, 2839–2861, doi:10.1175/JAS3980, http://dx.doi.org/10.1175/JAS3980, 2007.

Morrison, H. and Grabowski, W. W.: A Novel Approach for Representing Ice Microphysics in Models: Description and Tests Using a Kinematic Framework, Journal of the Atmospheric Sciences, 65, 1528–1548, 2008.

Morrison, H. and Grabowski, W. W.: Cloud-system resolving model simulations of aerosol indirect effects on tropical deep convection and its thermodynamic environment, Atmospheric Chemistry and Physics, 11, 10 503–10 523, 2011.

Morrison, H. and Milbrandt, J.: Comparison of Two-Moment Bulk Microphysics Schemes in Idealized Supercell Thunderstorm Simulations, Mon. Wea. Rev., 139, 1103–1130, doi:10.1175/2010MWR3433.1, 2011.

Morrison, H. and Milbrandt, J. A.: Parameterization of Cloud Microphysics Based on the Prediction of Bulk Ice Particle Properties. Part I: Scheme Description and Idealized Tests, Journal of the Atmospheric Sciences, 72, 287–311, 2015.

Morrison, H. and Pinto, J.: Mesoscale Modeling of Springtime Arctic Mixed-Phase Stratiform Clouds Using a New Two-Moment Bulk Microphysics Scheme, J. Atmos. Sci., 62, 3683—-3704, doi:http://dx.doi.org/10.1175/JAS3564.1, 2005.

Morrison, H. and Pinto, J.: Intercomparison of Bulk Cloud Microphysics Schemes in Mesoscale Simulations of Springtime Arctic Mixed-Phase Stratiform Clouds, Mon. Wea. Rev., 134, 1880–190, doi:http://dx.doi.org/10.1175/MWR3154.1, 2006.

Morrison, H., Curry, J., and Khvorostyanov, V.: A new double-moment microphysics parameterization for application in cloud and climate models. Part I: Description, J. Atmos. Sci., 62, 1665–1677, 2005.

Morrison, H., Thompson, G., and Tatarskii, V.: Impact of Cloud Microphysics on the Development of Trailing Stratiform Precipitation in a Simulated Squall Line: Comparison of One- and Two-Moment Schemes, Mon. Wea. Rev., 137, 991–1007, doi:10.1175/2008MWR2556.1, 2009.

Morrison, H., Milbrandt, J. A., Bryan, G. H., Ikeda, K., Tessendorf, S. A., and Thompson, G.: Parameterization of Cloud Microphysics Based on the Prediction of Bulk Ice Particle Properties. Part II: Case Study Comparisons with Observations and Other Schemes, Journal of the Atmospheric Sciences, 72, 312–339, 2015a.

Morrison, H., Morales, A., and Villanueva-Birriel, C.: Concurrent Sensitivities of an Idealized Deep Convective Storm to Parameterization of Microphysics, Horizontal Grid Resolution, and Environmental Static Stability, Mon. Wea. Rev., 143, 2082—2104, doi:http://dx.doi.org/10.1175/MWR-D-14-00271.1, 2015b.

Noppel, H., Blahak, U., Seifert, A., and Beheng, K. D.: Simulations of a hailstorm and the impact of {CCN} using an advanced two-moment cloud microphysical scheme, Atmospheric Research, 96, 286 –301, 2010.

Paulson, C.: The mathematical representation of wind speed and temperature profiles in the unstable atmospheric surface layer, Journal of Applied Meteorology, 9, 857–861, 1970.

Potvin, C. and Flora, M.: Sensitivity of Idealized Supercell Simulations to Horizontal Grid Spacing: Implications for Warn-on-Forecast, Mon. Wea. Rev., 143, 2998—-3024, doi:http://dx.doi.org/10.1175/MWR-D-14-00416.1, 2015.

Rajeevan, M., Kesarkar, A., Thampi, S. B., Rao, T., Radhakrishna, B., and Rajasekhar, M.: Sensitivity of {WRF} cloud microphysics to simulations of a severe thunderstorm event over Southeast India, Ann. Geophys., 28, 603—-619, 2010.

Rauber, R., Ochs, H. I., Di Girolamo, L., Göke, S., Snodgrass, E., Stevens, B., Knight, C., Jensen, J. B., Lenschow, D. H., Rilling, R. A., Rogers, D. C., Stith, J. L., Albrecht, B. A., Zuidema, P., Blyth, A. M., Fairall, C. W., Brewer, W. A., Tucker, S., Lasher-Trapp, S. G., Mayol-Bracero, O. L., Vali, G., Geerts, B., Anderson, J. R., Baker, B. A., Lawson, R. P., Bandy, A. R., Thornton, D. C., Burnet, E., Brenguier, J.-L., Gomes, L., Brown, P. R. A., Chuang, P., Cotton, W. R., Gerber, H., Heikes, B. G., Hudson, J. G., Kollias, P., Krueger, S. K., Nuijens, L., O'Sullivan, D. W., Siebesma, A. P., and Twohy, C. H.: Rain in shallow cumulus over the ocean: the RICO campaign, Bull. Amer. Meteor. Soc., 88, 1912–1928, 2007.

Rosenfeld, D., Lohmann, U., Raga, G., O'Dowd, C., Kulmala, M., Fuzzi, S., Reissell, A., and M.O., A.: Flood or Drought: How Do Aerosols Affect Precipitation?, Science, 321, 1309–1313, 2008.

Rutledge, S. and Hobbs, P.: The mesoscale and microscale structure and organisation of clouds and precipitation in midlatitude cyclones. VIII: A model for the seeder-feeder process in warm frontal rainbands., J. Atmos. Sci., 40, 1185–1206, 1983.

Saleeby, S. M. and van den Heever, S. C.: Developments in the CSU-RAMS Aerosol Model: Emissions, Nucleation, Regeneration, Deposition, and Radiation, Journal of Applied Meteorology and Climatology, 52, 2601–2622, doi:10.1175/JAMC-D-12-0312.1, http://dx.doi.org/10.1175/JAMC-D-12-0312.1, 2013.

Seifert, A. and Beheng, K. D.: A two-moment cloud microphysics parameterization for mixed-phase clouds. Part 2: Maritime vs. continental deep convective storms, Meteorology and Atmospheric Physics, 92, 67–82, doi:10.1007/s00703-005-0113-3, http://dx.doi.org/10.1007/s00703-005-0113-3, 2006a.

Seifert, A. and Beheng, K. D.: A two-moment cloud microphysics parameterization for mixed-phase clouds. Part 2: Maritime vs. continental deep convective storms, Meteorology and Atmospheric Physics, 92, 67–82, 2006b.

Seifert, A., Köhler, C., and Beheng, K. D.: Aerosol-cloud-precipitation effects over Germany as simulated by a convective-scale numerical weather prediction model, Atmospheric Chemistry and Physics, 12, 709–725, 2012.

Shipway, B. J. and Hill, A. A.: Diagnosis of systematic differences between multiple parametrizations of warm rain microphysics using a kinematic framework, Quarterly Journal of the Royal Meteorological Society, 138, 2196–2211, doi:10.1002/qj.1913, http://dx.doi.org/10.1002/qj.1913, 2012.

Skamarock, W., Klemp, J., Dudhia, J., Gill, D., Barker, D., Duda, M., Huang, X., Wang, W., and Powers, J.: A Description of the Advanced Research WRF Version 3 NCAR Technical Note June 2008, Tech. Rep. TN-475+STR, NCAR, National Center for Atmospheric Research, Box 3000, Boulder, Colorado 80307, USA, 2008.

Stevens, B. and Feingold, G.: Untangling aerosol effects on clouds and precipitation in a buffered system, Nature, 461, 607–613, 2009.

Stevens, B., Feingold, G., Cotton, W., and Walko, R.: Elements of the Microphysical Structure of Numerically Simulated Nonprecipitating Stratocumulus, J. Atmos. Sci., 53, 980—-1006, 1996.

Tao, W.-K., Li, X., Khain, A., Matsui, T., Lang, S., and Simpson, J.: Role of atmospheric aerosol concentration on deep convective precipitation: Cloud-resolving model simulations, Journal of Geophysical Research: Atmospheres, 112, 2007.

Tao, W.-K., Chen, J.-P., Li, Z., Wang, C., and Zhang, C.: Impact of aerosols on convective clouds and precipitation, Reviews of Geophysics, 50, 2012.

Thompson, G. and Eidhammer, T.: A Study of Aerosol Impacts on Clouds and Precipitation Development in a Large Winter Cyclone, Journal of the Atmospheric Sciences, 71, 3636–3658, 2014.

Thompson, G., Rasmussen, R., and Manning, K.: Explicit Forecasts of Winter Precipitation Using an Improved Bulk Microphysics Scheme. Part I: Description and Sensitivity Analysis, Mon. Wea. Rev., 132, 519–542, doi:10.1175/1520-0493(2004)132<0519:EFOWPU>2.0.CO;2, 2004.

Thompson, G., Field, P., Rasmussen, R., and Hall, W.: Explicit Forecasts of Winter Precipitation Using an Improved Bulk Microphysics Scheme. Part II: Implementation of a new snow parameterization, Mon. Wea. Rev., 136, 5095–5115, 2008.

Thompson, G., Tewari, M., Ikeda, K., Tessendorf, S., Weeks, C., Otkin, J., and Kong, F.: Explicitly-coupled cloud physics and radiation parameterizations and subsequent evaluation in {WRF} high-resolution convective forecasts, Atmospheric Research, 168, 92 – 104, doi:http://dx.doi.org/10.1016/j.atmosres.2015.09.005, http://www.sciencedirect.com/science/article/pii/S0169809515002835, 2016.

Tzivion, S., Feingold, G., and Levin, Z.: An Efficient Numerical Solution to the Stochastic Collection Equation, Journal of the Atmospheric Sciences, 44, 3139–3149, doi:10.1175/1520-0469(1987)044<3139:AENSTT>2.0.CO;2, http://dx.doi.org/10.1175/1520-0469(1987)044<3139:AENSTT>2.0.CO;2, 1987.

van den Heever, S., Carrió, G., Cotton, W., DeMott, P., and Prenni, A.: Impacts of Nucleating Aerosol on Florida Storms. Part I: Mesoscale Simulations, J. Atmos. Sci., 63, 1752–1775, 2006.

van Zanten, M. C., Stevens, B., Nuijens, L., Siebesma, A. P., Ackerman, A. S., Burnet, F., Cheng, A., Couvreux, F., Jiang, H., Khairoutdinov, M., Kogan, Y., Lewellen, D. C., Mechem, D., Nakamura, K., Noda, A., Shipway, B. J., Slawinska, J., Wang, S., and Wyszogrodzki, A.: Controls on precipitation and cloudiness in simulations of trade-wind cumulus as observed during RICO, Journal of Advances in Modeling Earth Systems, 3, doi:10.1029/2011MS000056, http://dx.doi.org/10.1029/2011MS000056, m06001, 2011.

Wang, Y., Fan, J., Zhang, R., Leung, L. R., and Franklin, C.: Improving bulk microphysics parameterizations in simulations of aerosol effects, Journal of Geophysical Research: Atmospheres, 118, 5361–5379, doi:10.1002/jgrd.50432, http://dx.doi.org/10.1002/jgrd.50432, 2013.

Washington, R., James, R., Pearce, H., Pokam, W., and Moufouma-Okia, W.: Congo Basin rainfall climatology: can we believe the climate models?, Phil. Trans. R. Soc. B, 368, 2013.

Webb, E.: Profile relationships: The log-linear range, and extension to strong stability, Quarterly Journal of the Royal Meteorological Society, 96, 67–90, 1970.

Weisman, M. and Klemp, J.: The Dependence of Numerically Simulated Convective Storms on Vertical Wind Shear and Buoyancy, Mon. Wea. Rev., 110, 504–520, 1982.

Weisman, M. and Klemp, J.: The structure and classification of numerically simulated convective storms in directionally varying wind shears, Mon. Wea. Rev., 112, 2479–2498, 1984.

Weisman, M. and Rotunno, R.: The use of vertical wind shear versus helicity in interpreting supercell dynamics, J. Atmos. Sci., 57, 1452–1472, 2000.

Weverberg, K. V., Vogelmann, A. M., Lin, W., Luke, E. P., Cialella, A., Minnis, P., Khaiyer, M., Boer, E. R., and Jensen, M. P.: The Role of Cloud Microphysics Parameterization in the Simulation of Mesoscale Convective System Clouds and Precipitation in the Tropical Western Pacific, Journal of the Atmospheric Sciences, 70, 1104–1128, 2013.

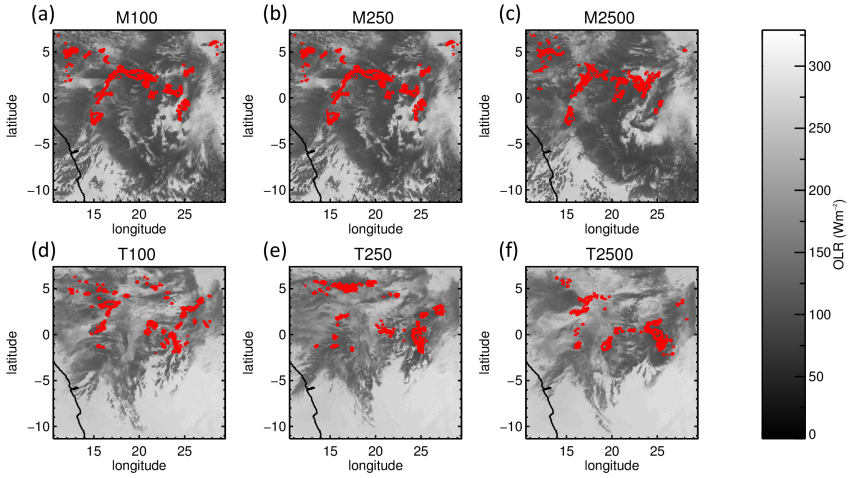

Figure 1. Congo case: Instantaneous outgoing longwave radiation (W m^2, greyscale) and 5 mm hr^{-1} surface precipitation rate (red contour) at 0700 UTC, 7 August 2007 in the Congo basin configuration. (a), (b) and (c) show CONGO-MORR simulations, (d), (e) and (f) show CONGO-THOM simulations. Prescribed CDNC values of 100, 250 and 2500 cm^{-3} are shown in (a, d), (b, e), and (c, f) respectively.

Weverberg, K. V., Goudenhoofdt, E., Blahak, U., Brisson, E., Demuzere, M., Marbaix, P., and van Ypersele, J.-P.: Comparison of one-moment and two-moment bulk microphysics for high-resolution climate simulations of intense precipitation, Atmospheric Research, 147–148, 145 – 161, 2014.

Wu, L. and Petty, G. W.: Intercomparison of Bulk Microphysics Schemes in Model Simulations of Polar Lows, Monthly Weather Review, 138, 2211–2228, doi:10.1175/2010MWR3122.1, 2010.

Yamaguchi, T. and Feingold, G.: Technical note: Large-eddy simulation of cloudy boundary layer with the Advanced Research WRF model, Journal of Advances in Modeling Earth Systems, 4, doi:10.1029/2012MS000164, http://dx.doi.org/10.1029/2012MS000164, m09003, 2012.

Zhang, J., Reid, J. S., and Holben, B. N.: An analysis of potential cloud artifacts in MODIS over ocean aerosol optical thickness products, Geophysical Research Letters, 32, 2005.

Zhang, S., Wang, M., Ghan, S. J., Ding, A., Wang, H., Zhang, K., Neubauer, D., Lohmann, U., Ferrachat, S., Takeamura, T., Gettelman, A., Morrison, H., Lee, Y., Shindell, D. T., Partridge, D. G., Stier, P., Kipling, Z., and Fu, C.: On the characteristics of aerosol indirect effect based on dynamic regimes in global climate models, Atmospheric Chemistry and Physics, 16, 2765–2783, doi:10.5194/acp-16-2765-2016, http://www.atmos-chem-phys.net/16/2765/2016/, 2016.

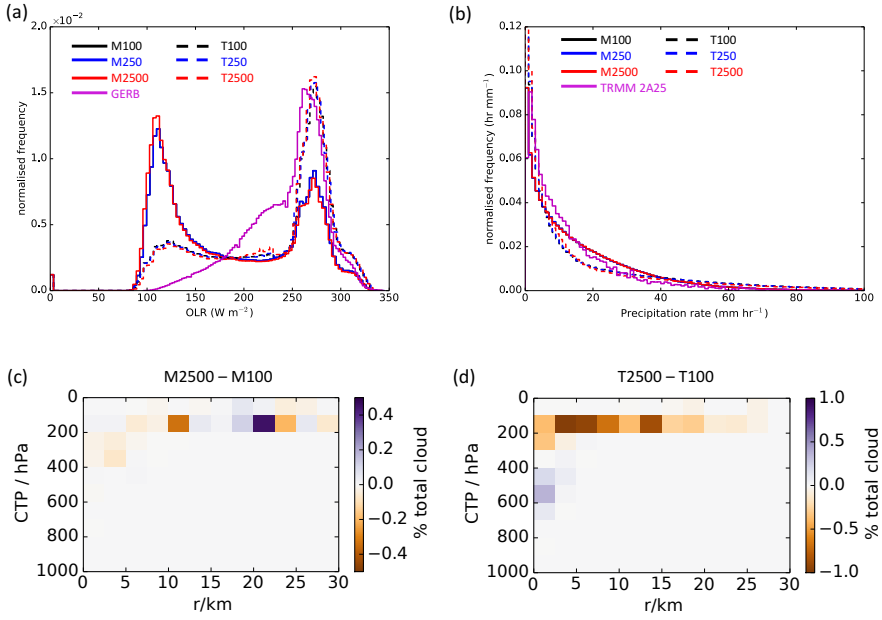

Figure 2. Congo case: (a) frequency distributions of OLR from the WRF simulations and observations from GERB over the period 01 to 10 August 2007 , (b) self-weighted precipitation rate distributions from the WRF simulations and observations from the ungridded TRMM 2A25 product, which has a similar spatial resolution to the 4 km model grid length~~.~~, (c) difference in the joint distribution of cloud top pressure in updraughts (identified by masking points where the maximum vertical velocity exceeds 1 ms^{-1}, and then applying a connected-components labelling algorithm to identify unique updraught areas) and horizontal radius of updraughts when CDNC is increased from 100 to 1000 cm^{-3} using the Morrison microphysics scheme, (d) difference in the joint distribution of cloud top pressure in updraughts and horizontal radius of updraughts when CDNC is increased from 100 to 1000 cm^{-3} using the Thompson microphysics scheme

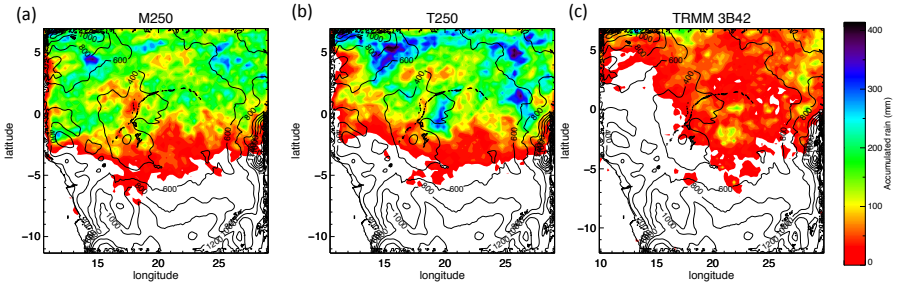

Figure 3. Congo case: accumulated surface precipitation (mm) from 01 to 10 August 2007 in the Congo basin, showing data from (a) CONGO-M250, (b) CONGO-T250 and (c) observations from the TRMM 3B42 gridded 3-hourly mean merged precipitation product. The simulation data shown in this Figure has been coarsened to the 0.25°spatial resolution of the TRMM product.

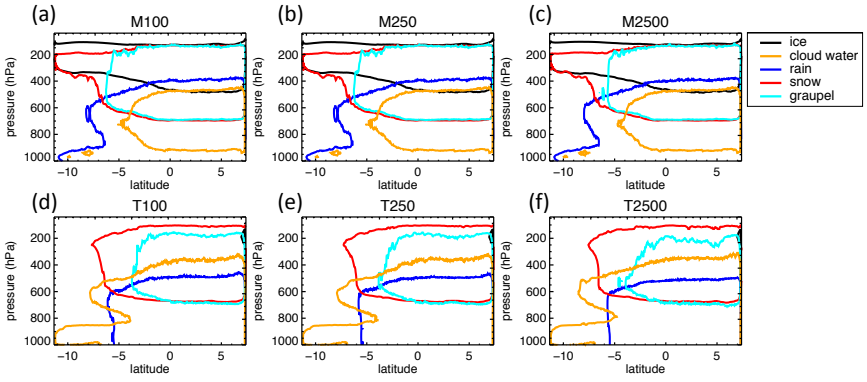

Figure 4. Congo case: Zonal mean vertical sections of hydrometeor classes (colour contours) from 01 to 10 August 2007. Hydrometeor mass mixing ratios are contoured at 10^{-6} kg kg^{-1}.

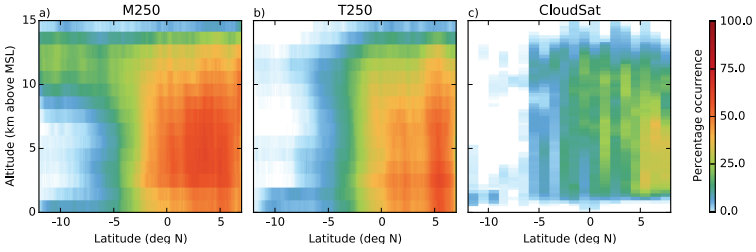

Figure 5. Congo case: 10-day histogram for the period 1–10 August 2007 of model reflectivities derived from hydrometeor fields passed through the Quickbeam radar simulator (Haynes et al., 2007), thresholded at values greater than -20 dBZ for (a) CONGO-M250, (b) CONGO-T250, and (c) ~~equivalent histogram produced from climatology data from~~ the CloudSat 2B-GEOPROF product~~from August 2006–2010 inclusive~~. In (a) and (b) the models have been sampled at the times of the nearest CloudSat overpasses.

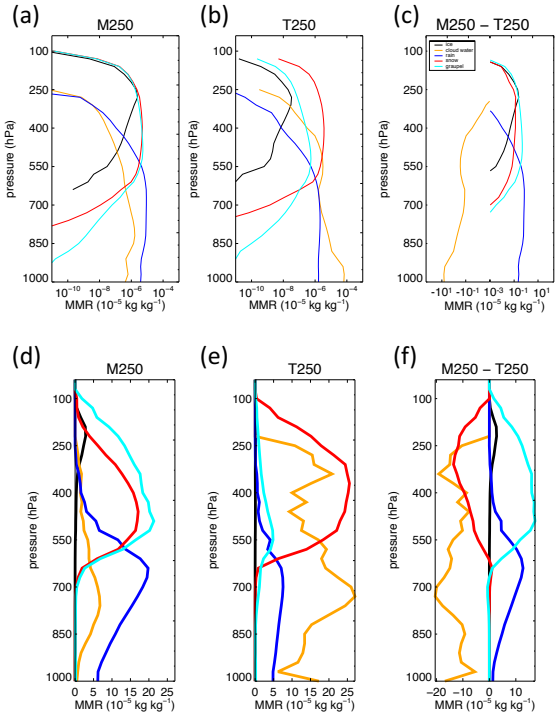

Figure 6. Congo case: ~~Domain-mean~~ Mean vertical profiles of hydrometeor mass mixing ratios (MMR) averaged over the period 1–10 August 2007. (a) CONGO-M250 domain-mean, (b) CONGO-T250 ~~and~~ domain-mean, (c) the difference in the domain-mean hydrometeor mixing ratio profiles (CONGO-M250 minus CONGO-T250), (d) CONGO-M250 mean over condensed points only, (e) CONGO-T250 mean over condensed points only for each hydrometeor class, and (f) the difference in the condensate-mean hydrometeor mixing ratio profiles (CONGO-M250 minus CONGO-T250). Note the logarithmic horizontal axis used in (a), (b) and (c) due to the total difference between the hydrometeor classes simulated by the two schemes spanning several orders of magnitude.

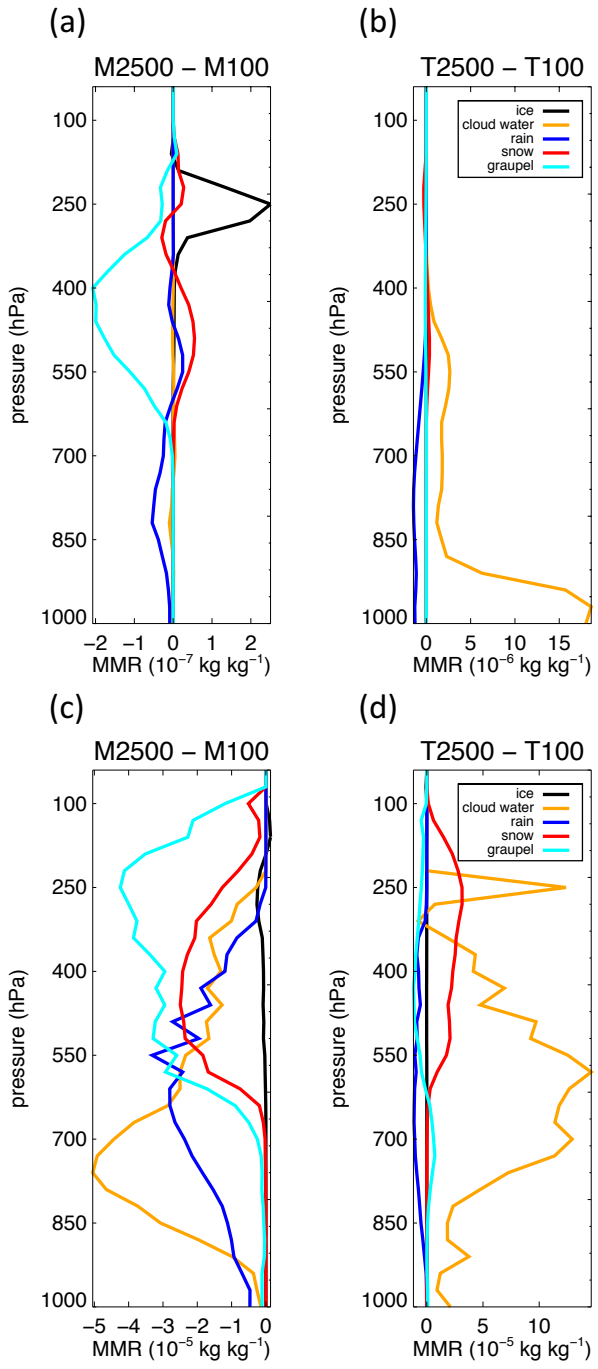

Figure 7. Congo case: Difference in the ~~domain-mean~~ mean hydrometeor mixing ratio profiles under polluted and pristine conditions averaged over the period 1–10 August 2007. (a) CONGO-M2500 domain-mean minus CONGO-M100 ~~and~~ domain-mean, (b) CONGO-T2500 domain-mean minus CONGO-T100 ~~. Note the difference in order of magnitude in the scale in~~ domain-mean, (ac) ~~CONGO-MORR~~ CONGO-M2500 mean over all condensed points of each hydrometeor class minus CONGO-M100 mean over all condensed points, and (~~10^{-7} kg kg^{-1}~~d) ~~compared to (b) CONGO-THOM (10^{-6} kg kg^{-1})~~ CONGO-T2500 mean over all condensed points minus CONGO-T100 mean over all condensed points.

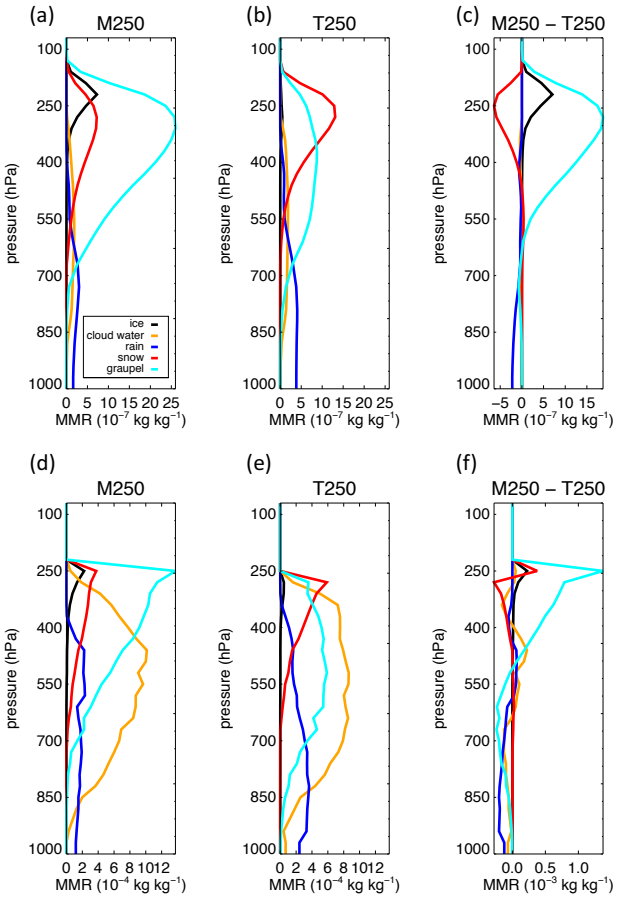

Figure 8. Idealised supercell: ~~Domain-mean~~ Mean vertical profiles of hydrometeor mass mixing ratios (MMR), as Figure 6, averaged over the 2 h of the supercell simulation. (a) SUPER-M250 domain-mean, (b) SUPER-T250 domain-mean, (c) SUPER-M250 domain-mean minus SUPER-T250 domain-mean, (d) SUPER-M250 condensate-mean of each hydrometeor class, (e) SUPER-T250 condensate-mean, (c) SUPER-M250 condensate-mean minus SUPER-T250 condensate-mean.

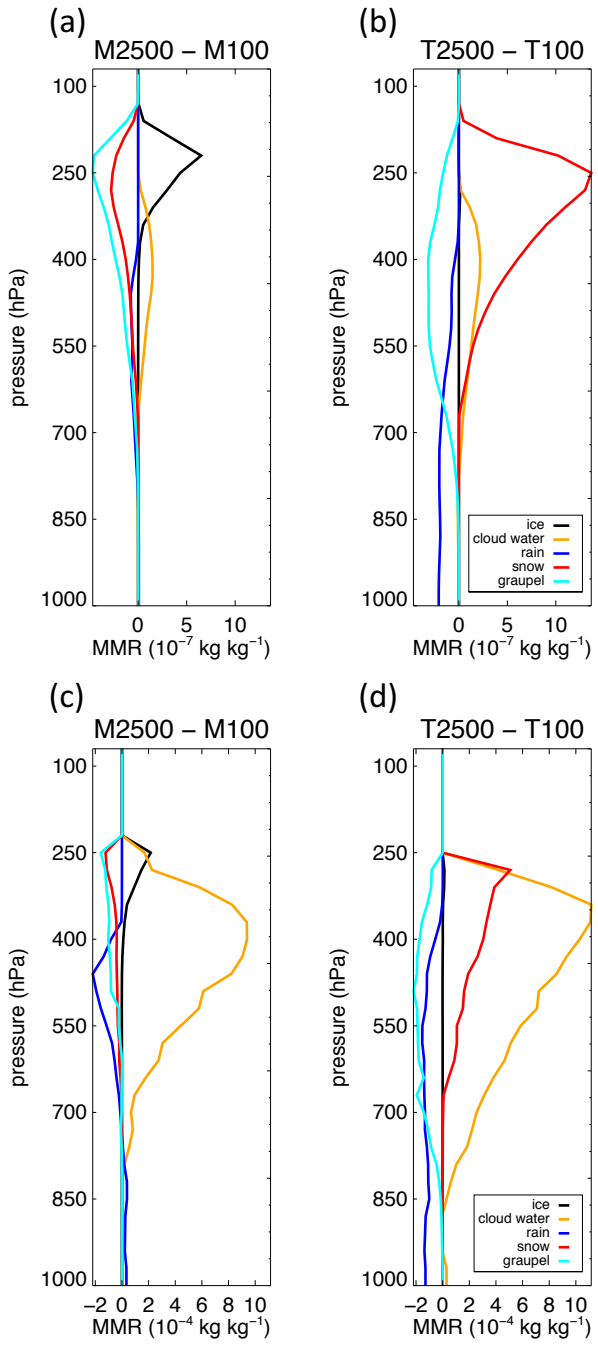

Figure 9. Idealised supercell: difference in the ~~domain-mean~~ mean hydrometeor mixing ratio profiles under polluted and pristine conditions, as Figure 7, averaged over the 2 h of the supercell simulation. (a) SUPER-M2500 domain-mean minus SUPER-M100 ~~and~~ domain-mean, (b) SUPER-T2500 domain-mean minus SUPER-T100 domain-mean, (c) SUPER-M2500 condensate-mean of each hydrometeor class minus SUPER-M100 condensate-mean, and (d) SUPER-T2500 condensate-mean minus SUPER-T100 condensate-mean.

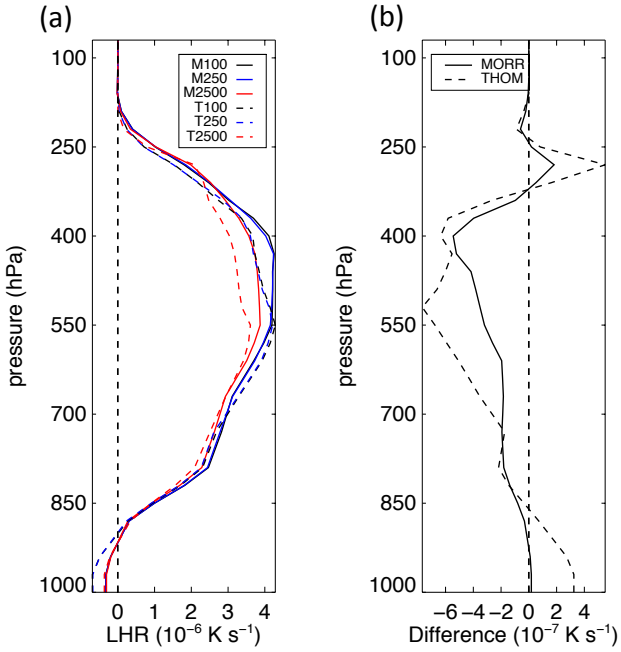

Figure 10. Idealised supercell: (a) Vertical profiles of domain-mean total latent heating rate (LHR) over the 2 h of the supercell simulation for SUPER-MORR and SUPER-THOM for CDNC values of 100, 250 and 2500 cm^{-3}. (b) Difference in the total latent heating contributions over the 2 h of the supercell simulation for SUPER-M2500 minus SUPER-M100 and SUPER-T2500 minus SUPER-T100.

Table 1. List of model configurations

Model settings	**Congo**	**Supercell**	**RICO LES**
horizontal grid length (km)	4	4	0.1
number of grid points (W–E and S–N)	525	400	129
number of vertical levels	30	30	100
model top	5000 Pa	20 km	4 km
time step (s)	12	12	1
simulation length	10 days	2 hours	24 hours
LW radiation scheme	RRTM	-	-
SW radiation scheme	Goddard	-	-
PBL scheme	YSU	-	-

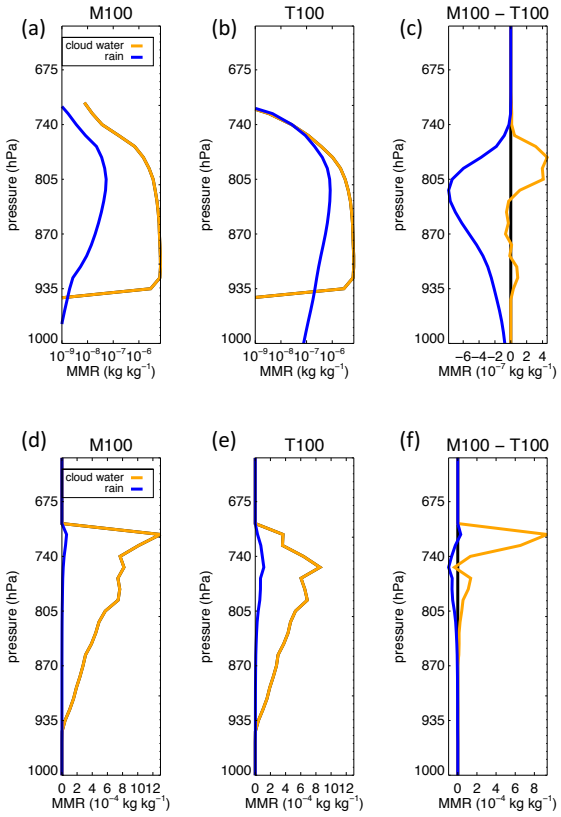

Figure 11. RICO case: ~~Domain-mean~~ Mean vertical profiles of hydrometeor mass mixing ratios (MMR), as Figure 6, averaged over the 24 h of the RICO simulation. (a) RICO-M100 domain-mean, (b) RICO-T100 domain-mean, (c) RICO-M100 domain-mean minus RICO-T100 domain-mean, (d) RICO-M100 condensate-mean over each hydrometeor class, (eb) RICO-T100 condensate-mean, (f) RICO-M100 condensate-mean minus RICO-T100 condensate-mean. Note that because the rain amounts are very small, especially in M100, (a) and (b) are shown with a logarithmic horizontal axis.

Table 2. List of microphysics configurations tested, and the abbreviations used for each run

Prescribed CDNC	Congo MORR	Congo THOM	Supercell MORR	Supercell THOM	RICO MORR	RICO THOM
100 cm^{-3}	CONGO-M100	CONGO-T100	SUPER-M100	SUPER-T100	RICO-M100	RICO-T100
250 cm^{-3}	CONGO-M250	CONGO-T250	SUPER-M250	SUPER-T250	RICO-M250	RICO-T250
2500 cm^{-3}	CONGO-M2500	CONGO-T2500	SUPER-M2500	SUPER-T2500	RICO-M2500	RICO-T2500

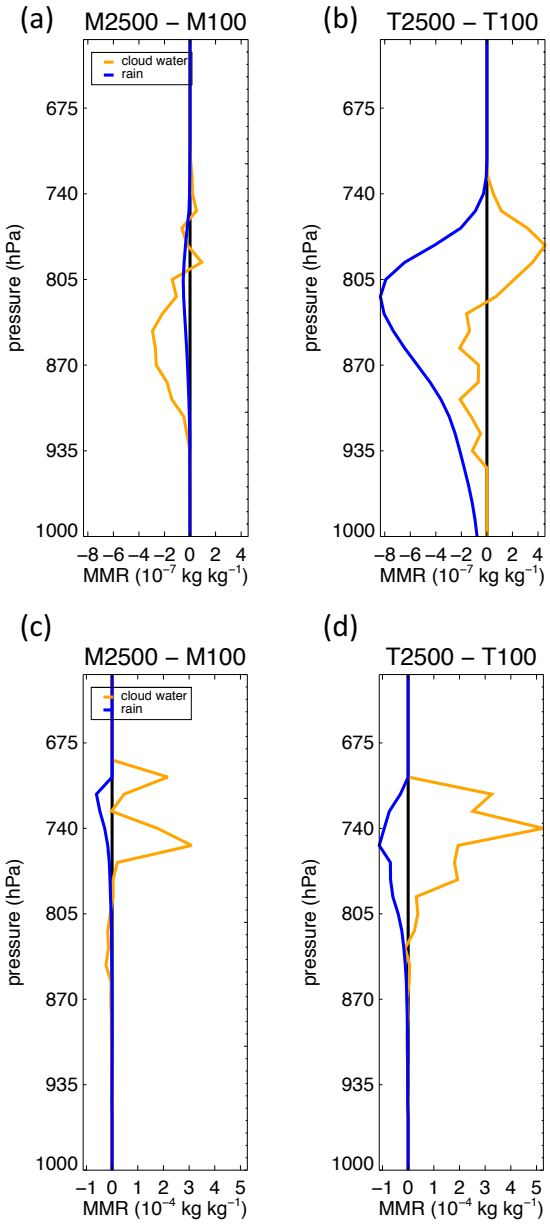

Figure 12. RICO case: difference in the ~~domain-mean~~ mean hydrometeor mixing ratio profiles under polluted and pristine conditions, as Figure 7, averaged over the 24 h of the RICO simulation. (a) RICO-M2500 domain-mean minus RICO-M100 domain-mean, (b) RICO-T2500 domain-mean minus RICO-T100 domain-mean, (c) RICO-M2500 condensate-mean over each hydrometeor class minus RICO-M100 condensate-mean, (d) RICO-T2500 condensate-mean minus RICO-T100 condensate-mean

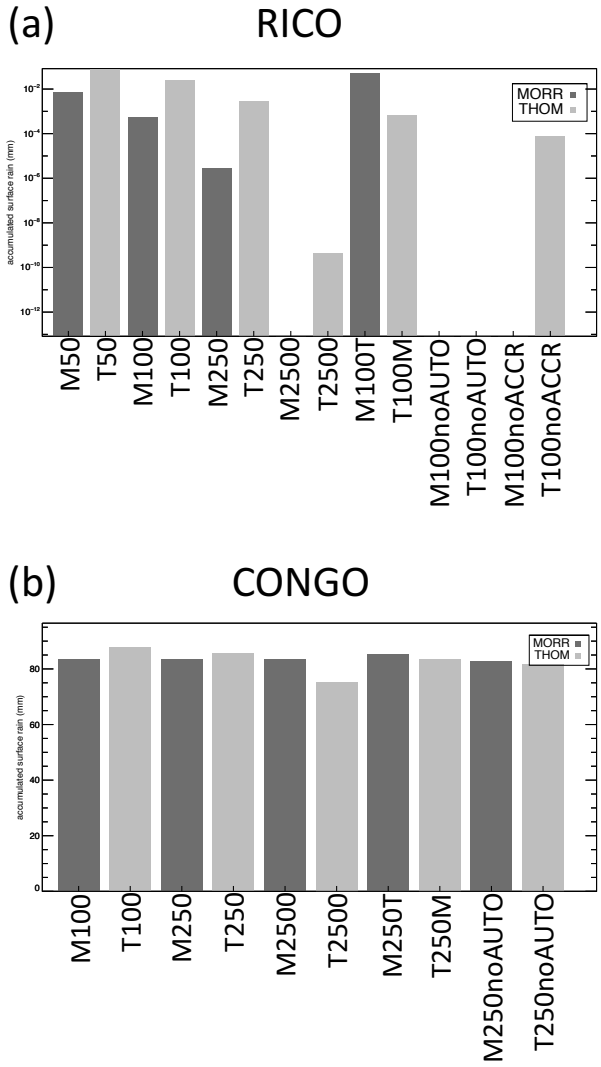

Figure 13. Total accumulated surface rain (mm) for each of the microphysics simulations, including a series of sensitivity simulations, for (a) RICO case, total after 24 h of simulation, (b) Congo case, total over the period 1–10 August 2007. Note that because the magnitude of the rain response to CDNC differs so strongly between the configurations in the RICO case, a logarithmic vertical axis is used in (a). The horizontal dashed line in (b) indicates the total precipitation from the TRMM 2A25 product over the same period.

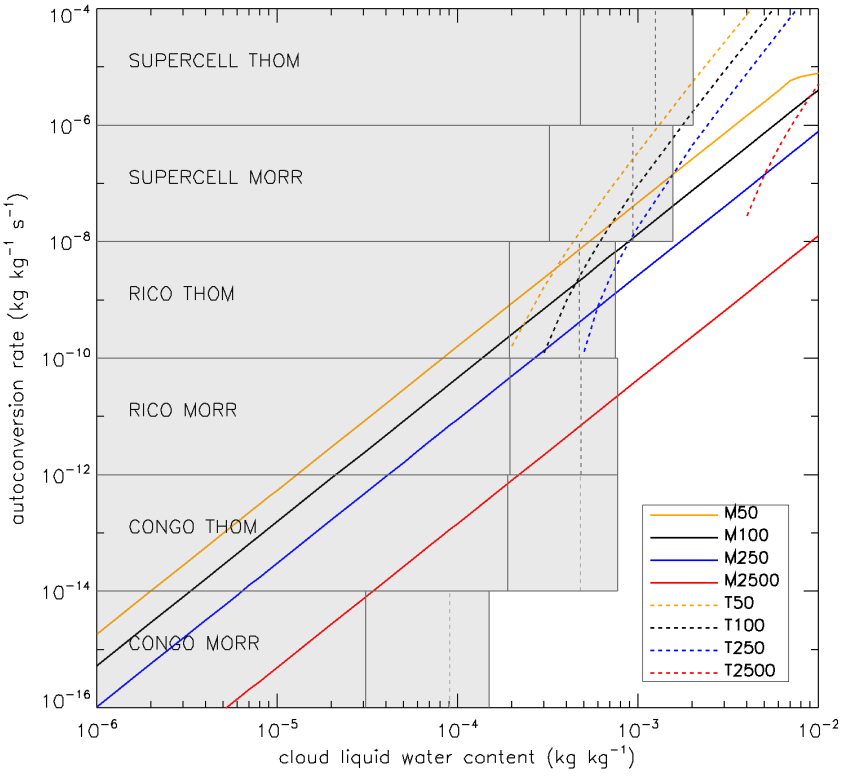

Figure 14. Autoconversion rate as a function of cloud water content for the MORR and THOM microphysics schemes (solid and dashed lines respectively) for super-pristine, pristine, moderately polluted and polluted conditions. Also shown are labelled grey bars showing the mean (solid vertical grey line) and 1 and 2 standard deviations (dashed vertical grey line and end of bar, respectively) cloud water content averaged over all prescribed CDNC configurations for each case (note that the variability in mean cloud water content with CDNC is significantly less than the variability due to microphysics scheme).

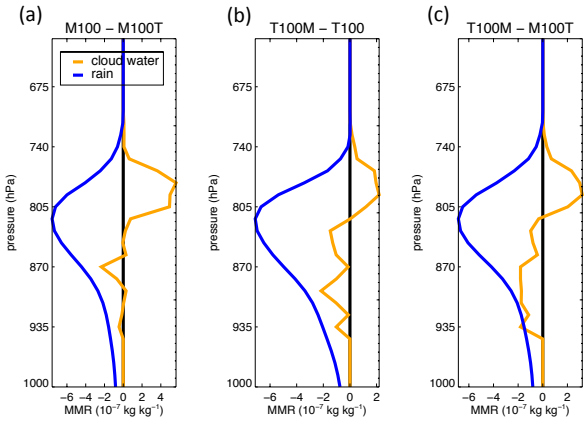

Figure 15. RICO case: Difference in the domain-mean vertical profiles of hydrometeor mass mixing ratios (MMR) between MORR and THOM, as Figure 11c, averaged over the 24 h of the RICO simulation for the configurations with the autoconversion treatment swapped between the microphysics schemes: (a) M100 minus M100T, (b) T100M minus T100, (c) T100M minus M100T

Table 3. Maximum relative difference of domain-mean hydrometeor mass mixing ratio profiles for the MORR and THOM schemes. The relative change in the hydrometeor mass mixing ratios are computed in each case for ~~T250 compared to~~ M250 minus T250.

difference	**CONGO**	**SUPERCELL**	**RICO**
liquid cloud mass	-10900 %	-58.3 %	+17.0 %
ice mass	+98.7 %	+96.9 %	N/A
rain mass	+82.2 %	-138 %	-3830 %
snow mass	+40.8 %	-99.8 %	N/A
graupel mass	+91.6 %	+72.7 %	N/A

Table 4. Maximum relative difference of response of model configurations to polluted conditions. The relative change in the ~~hydrometeor~~ domain-mean rehydrometeor mass mixing ratios are computed in each case for CDNC values of 2500 cm^{-3} ~~compared to~~ minus 100 cm^{-3}.

difference	**CONGO-MORR**	**CONGO-THOM**	**SUPER-MORR**	**SUPER-THOM**	**RICO-MORR**	**RICO-THOM**
liquid cloud mass	-0.59 %	+32.2 %	+146 %	+169 %	-5.21 %	+44.0 %
ice mass	+12.5 %	-5.61 %	+116 %	+29.7 %	N/A	N/A
rain mass	-0.67 %	-62.6 %	-93.7 %	-51.6 %	-100 %	-100 %
snow mass	+1.37 %	+13.8 %	-33.5 %	+109 %	N/A	N/A
graupel mass	-4.60 %	-29.9 %	-19.1 %	-36.7 %	N/A	N/A

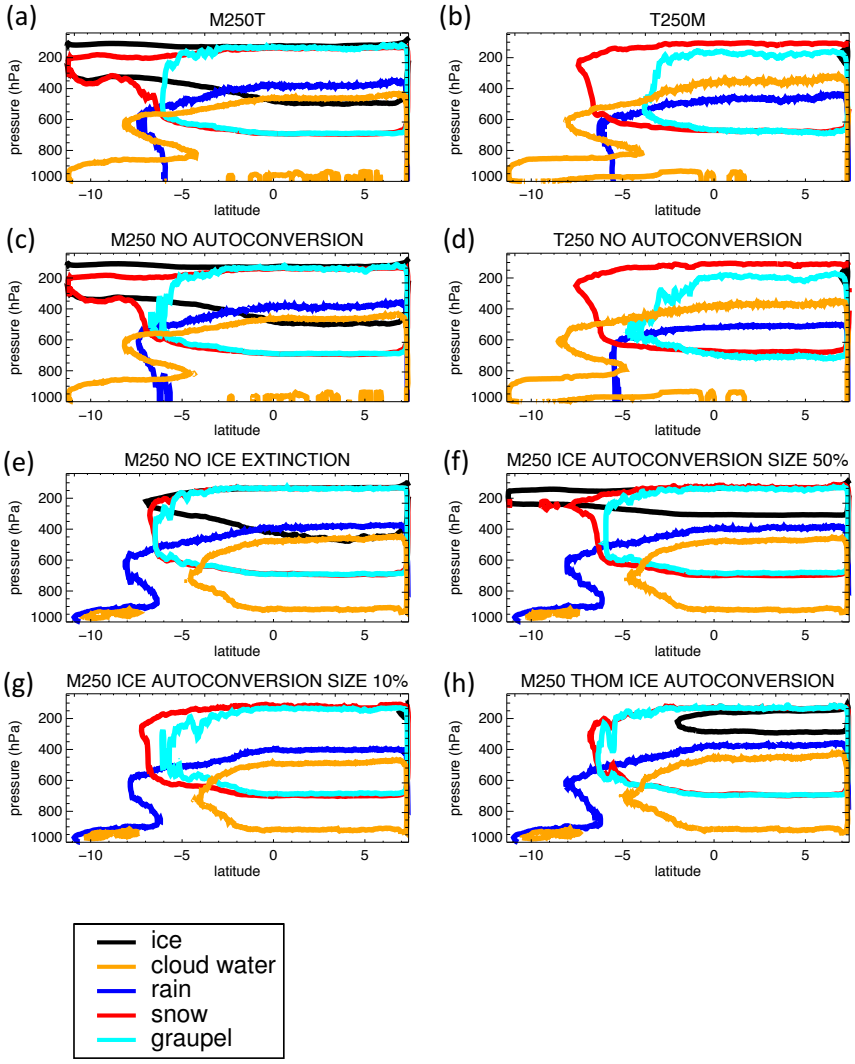

Figure 16. Congo case: Zonal mean vertical sections of hydrometeor classes (colour contours) from 01 to 10 August 2007, as Figure 4, but for the configurations with the autoconversion treatment swapped between the microphysics schemes, (a) CONGO-M250T and (b) CONGO-T250M, and for the configurations with (c) CONGO-M250 with autoconversion turned off, (d) CONGO-T250 with autoconversion turned off, (e) CONGO-M250 with the ice extinction coefficient set to zero in the longwave and shortwave radiation schemes, (f) CONGO-M250 with the threshold size parameter for conversion of ice to snow reduced to 50% of its default value, (g) CONGO-M250 with the threshold size parameter for conversion of ice to snow reduced to 10% of its default value, (h) CONGO-M250 with the autoconversion of ice to snow replaced by that used in the Thompson microphysics scheme. Hydrometeor mass mixing ratios are contoured at 10^{-6} kg kg^{-1}.